# CHAPTER 9

# RESULTS AND DISCUSSION ON MACHINE AND DEEP LEARNING METHODS FOR DISEASE PREDICTION

## 9.1 INTRODUCTION

Disease detection enables practitioners to make highly precise decisions regarding patients' health and their specific situation. ML methods present solutions to minimize errors in the forecast as well as appreciate symptoms for specific diseases. Diverse classification methods are employed to categorize disease data as well as forecast specific diseases or not. When the data reaches a certain level, the efficiency of conventional machine learning (ML) methods is significantly reduced. Therefore, DL methods are applied to solve this problem. In this research, novel machine learning (ML) and deep learning-based pre-processing, feature selection, and classification techniques are developed for disease forecasting. Overall, the database is divided into training and testing sets, where eighty percent of the patient data is used for training and twenty percent for testing. Additionally, the 70:30 splitting ratio is discussed in Section 9.6.

## 9.2 RESULTS AND DISCUSSION FOR PREPROCESSING

The proposed ALRTOHE technique and ZMFNE technique are compared with existing methods, such as the CNN-GRU-based hybrid deep learning (DL) method designed by Anil Utku (2023) and the Variant of Concerned Deep Learning (VOC-DL) prediction framework developed by Zhifang Liao *et al.* (2022). Results of both proposed preprocessing methods through conventional techniques are given in terms of tables and graphs.

### 9.2.1 Result of preprocessing accuracy

Preprocessing accuracy is referred in proportion to the amount of data samples that are properly preprocessed to the overall count of data taken from a given dataset. It is given below.

$$P_{Acc} = \frac{Nd_{cp}}{Td_{.}} * 100 \quad (9.1)$$

Where '$P_{Acc}$' point outs the preprocessing accuracy, '$Nd_{cp}$' point outs number of data correctly preprocessed as well as '$Td$' is total number of data. When accuracy of preprocessed data is high, the performance of proposed technqiue is said to be more efficient than the other methods.

### 9.2.2 Performance of Preprocessing Time

Preprocessing time is measured as the time taken to preprocessing given sample data. It is determined as given below.

$$PTime = \sum_{i=1}^{n} n * Time\ (psd) \quad (9.2)$$

From (9.2), '*PTime*' denotes the preprocessing time, '$n$' indicates number of sample data. '$Time[psd]$' represent sample data. It is calculated by milliseconds (ms).

### 9.2.3 Impact of Space complexity

An amount of memory required by an algorithm or process to run is referred as space complexity, typically expressed in size of input data. When space complexity is mentioned in kilobytes (KB), it is a measure of how much memory (in kilobytes) the algorithm uses. The results of space complexity in KB are obtained from experimental analysis. In mathematical term it is computed as given below.

$$S_c = \sum_{i=1}^{n} n * Mem(psd) \quad (9.3)$$

From the above equation, space complexity is calculated depend on product of several input data samples as well as space used for preprocessing single data. Where '$S_c$' refers space complexity, and '*Mem(*psd*)*' indicates number of patient data samples from dataset. It is computed in Megabytes (KB).

### 9.2.4 Performance of Error Rate

Error rate is referred as ratio of volume of patient information which incorrectly preprocessed to overall amount of data from dataset. It mathematically expressed as follows.

$$E_r = \frac{Nd_{ip}}{Td_.} * 100 \quad (9.4)$$

Where '$E_r$' denotes the error rate and '$Nd_{ip}$' indicates number of data samples incorrectly preprocessed. If error rate of preprocessed data is minimum, then result of proposed technqiue is more effective for disease detection.

**Table 9.1 (a): Results of Preprocessing Techniques for COVID-19 dataset**

| Methods/Metrics | Training PA (%) | Testing PA (%) | Preprocessing time (ms) | Error rate (%) | Space complexity (KB) |
|---|---|---|---|---|---|
| Existing VOC-DL | 70.99 | 68.54 | 6270 | 29.00 | 77.00 |
| Existing CNN-GRU based hybrid deep learning model | 75.19 | 72.62 | 5930 | 24.80 | 69.30 |
| Proposed ALRTOHE | 82.43 | 80.36 | 5430 | 17.56 | 64.70 |
| Proposed ZMFNE | 85.86 | 83.12 | 5060 | 14.13 | 60.00 |

**Table 9.1 (b): Results of Preprocessing Techniques for Pneumonia dataset**

| Methods/Metrics | Training PA (%) | Testing PA (%) | Preprocessing time (ms) | Error rate (%) | Space complexity (KB) |
|---|---|---|---|---|---|
| Existing VOC-DL | 73.72 | 69.25 | 6280 | 31.21 | 80 |
| Existing CNN-GRU based hybrid deep learning model | 78.91 | 74.62 | 5950 | 27.42 | 72 |
| Proposed ALRTOHE | 87.81 | 81.25 | 5450 | 19.17 | 68 |
| Proposed ZMFNE | 89.83 | 84.25 | 5090 | 16.23 | 65 |

Table 9.1 (a) and (b) describe the performance result of preprocessing techniques for the datasets COVID-19 and Pneumonia. The performance of the Preprocessing Accuracy (PA) of the proposed ALRTOHE technique and the ZMFNE technique is compared with that of an existing CNN-GRU-based hybrid deep learning (DL) method and VOC-DL. The table's mean value reveals which preprocessing accuracy of the ALRTOHE method and ZMFNE technique is

enhanced compared to the two existing techniques. Specifically, the ZMFNE technique yields higher preprocessing accuracy than the ALRTOHE technique. Similarly, the preprocessing time, error rate, and space complexity results are found to be the minimum in the proposed ZMFNE technique. From the Table 9.1 (a) and (b), the mean values of preprocessing accuracy in the training phase are obtained as 85.86%, 82.43%, 75.19%, and 70.99% for ZMFNE, ALRTOHE, CNN-GRU-based hybrid DL method, and VOC-DL, respectively, for the COVID-19 dataset. Similarly, PA values of 89.83%, 87.81%, 78.91%, and 73.72% are obtained for the Pneumonia dataset using the ZMFNE, ALRTOHE, CNN-GRU-based hybrid DL method, and VOC-DL, respectively. The exploratory evaluation results indicate that the accuracy of preprocessing is enhanced in the proposed ZMFNE technique compared to other methods.

The outlined ZMFNE technique performs diverse processes to provide the structured dataset. Initially, a sample input matrix is generated with rows and columns, depending on the patient data and features. After that, the normalization is performed for each sample through the zero mean feature scaling. These normalized data are transformed into a base-2 representation using the one-hot encoding method. With this, the input sample data are correctly preprocessed to enhance the accuracy. Thus, accuracy of the e training preprocessing is improved by 11% using the proposed ZMFNE technique evaluated against to the existing CNN-GRU-based hybrid deep learning (DL) method and by 15% compared to the existing VOC-DL. Compared values show that the proposed ZMFNE technique achieves a 15% reduction in preprocessing time compared to the existing CNN-GRU-based hybrid deep learning (DL) method and a 19% reduction compared to the existing VOC-DL. Additionally, the space complexity of the ZMFNE method is reduced by 13% and 22% compared to the CNN-GRU-based hybrid deep learning model and VOC-DL for the COVID-19 dataset.

The proposed ZMFNE technique achieved a lower error rate during preprocessing of the input dataset. This is due to the application of a zero-mean scaling-based normalization process and one-hot encoding data transformation. First, the scaling model is employed to normalize the data into a specific range. With this, the data transformation is performed using one-hot encoding, where the binary representation of the data is acquired. With this, the error rate is

minimized in the proposed ZMFNE technique by 11% compared to the existing CNN-GRU-based hybrid deep learning (DL) method and by 15% compared to the existing VOC-DL.

The experiment evaluation results identified that the preprocessing results are improved in the proposed ZMFNE technique compared to other methods, was evaluated using Equation (3.12). The training preprocessing accuracy is enhanced by 14% using the proposed ZMFNE technique evaluated against the existing CNN-GRU-based hybrid DL method and by 21% compared to the existing VOC-DL method, respectively, for the Pneumonia dataset. The preprocessing time is reduced by 21% using the proposed ZMFNE technique compared to the existing CNN-GRU-based hybrid deep learning (DL) method and by 27% compared to the existing VOC-DL method, respectively, for the Pneumonia dataset. The error rate associated with the ZMFNE method is reduced by 43% and 51% compared to the CNN-GRU-based hybrid deep learning method and the existing VOC-DL for the COVID-19 dataset. Additionally, the space complexity of the proposed ZMFNE technique is decreased by 52% and 61% compared to the CNN-GRU-based hybrid DL method and VOC-DL for the Pneumonia dataset.

### 9.2.5 Performance of ROC Curve for preprocessing

The disease prediction rate performance is measured using the ROC curve. With the help of the ROC curve, preprocessing is performed depending on whether a prediction is correctly or wrongly predicted. ROC curves are estimated with true positives and false positives. Table 9.1(c) shows the Tabulation for ROC Curve for Preprocessing.

**Table 9.1 (c) Tabulation for ROC Curve for preprocessing**

| False Positive Rate | True Positive Rate | | | |
|---|---|---|---|---|
| | Existing VOC-DL | Existing CNN-GRU based hybrid deep learning model | Proposed ALRTOHE | Proposed ZMFNE |
| 0.1 | 0 | 0 | 0 | 0 |
| 0.2 | 0.23 | 0.28 | 0.31 | 0.36 |
| 0.3 | 0.3 | 0.35 | 0.4 | 0.44 |
| 0.4 | 0.37 | 0.4 | 0.47 | 0.52 |
| 0.5 | 0.43 | 0.48 | 0.53 | 0.6 |
| 0.6 | 0.5 | 0.54 | 0.62 | 0.65 |
| 0.7 | 0.55 | 0.59 | 0.66 | 0.7 |
| 0.8 | 0.62 | 0.66 | 0.71 | 0.74 |
| 0.9 | 0.67 | 0.7 | 0.75 | 0.79 |
| 1 | 0.72 | 0.75 | 0.83 | 0.86 |

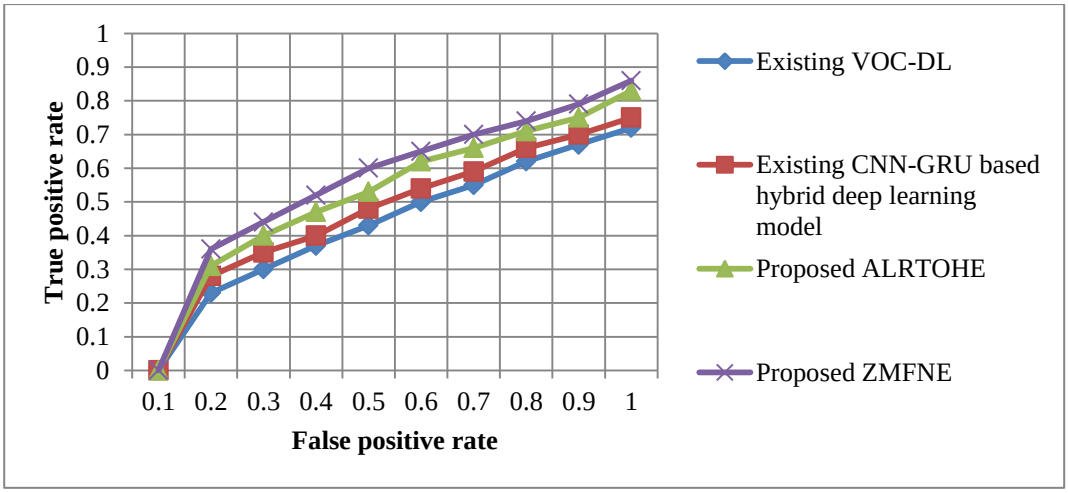


**Figure 9.1 Results of ROC Curve for preprocessing**

Figure 9.1 shows a visual representation of the ROC curve examination of the proposed and existing preprocessing ALRTOHE technique, ZMFNE technique, CNN-GRU-based hybrid deep learning model, and VOC-DL. Additionally, ROC performs an analysis of disease identification based on the true positive rate and false positive rate. From the above Figure, it is

representative that the ROC curve of the ZMFNE technique is relatively enhanced than existing methods.

## 9.3 RESULTS AND DISCUSSION FOR FEATURE SELECTION

Result evaluation of the Nonlinear Sammon Projective Pattern Selection (NSPPS) Model, Tversky Similarity-Indexed Distributive Feature Embedding (TSIDFE) technique and Statistical Correlative Targeted Projection Pursuit-based Feature Selection (SCTPP-FS) are compared with existing AHEG-FS model and hybrid Chi$^2$-MI based feature selection model.

### 9.3.1 Performance of Feature Selection Accuracy

Feature selection accuracy refers to the effectiveness of a feature selection process in identifying the most pertinent and informative aspects from a dataset that contribute significantly to the performance of a prognostic method. It is described as the proportion of the count of data features properly selected based on the overall number of data features considered as input. It is mathematically computed as follows.

$$\mathrm{FS}_{acc} = \frac{Ndf_{cs}}{T_{df}} * 100 \qquad (9.5)$$

Where '$FS_{acc}$' Feature Selection accuracy, '$Ndf_{cs}$' number of data feature correctly selected and '$T_{df}$' total number of data features. When accuracy of feature selection is improved, result of proposed method is improved.

### 9.3.2 Study of Feature Selection Time

Feature selection time is referred to as the amount of time used to select relevant feature data for disease detection. It is mathematically expressed as given below.

$$F_{st} = \sum_{i=1}^{n} Ndf_i * Time[sdf]. \qquad (9.6)$$

Where '$F_{st}$' indicates a feature selection time, '$Ndf_i$' indicates number of data feature samples for disease detection and '$Time\ [sdf]$' is a time for single data feature selection. It is calculated by milliseconds (ms).

### 9.3.3 Results of Space Complexity

Space complexity is evaluated as the memory capacity needed to choose the more informative pertinent features of patient data samples obtained from the input dataset. It is mathematically formulated as given below.

$$S_c = \sum_{i=1}^{n} Nd_i * Mem_{sfd} \quad (9.7)$$

Where '$SC$' denotes the space complexity and it is estimated based on the memory consumed for choosing pertinent features in data samples '$Mem_{sfd}$'. When there is a lower value of space complexity, the performance feature selection is improved. Space complexity is computed in kilobytes (KB).

### 9.3.4 Impact of Error Rate

Error rate is described as the proportion of the count of data feature wrongly selected to the total number of data feature from the dataset. It is arithmetically formulated given below.

$$E_r = \frac{Ndf_{ws}}{T_{df}} * 100 \quad (9.8)$$

In the above equation (9.8), '$E_r$' indicates the error rate and '$Ndf_{ws}$' represents the number of data feature wrongly selected. The performance of disease prediction is better when the error rate is smaller.

**Table 9.2 (a) Results of Feature Selection Techniques for COVID-19 dataset**

| Methods/Metrics | Training FA (%) | Testing FA (%) | Feature Selection time (ms) | Error rate (%) | Space complexity (KB) |
|---|---|---|---|---|---|
| Existing **Chi$^2$-MI** | 80.66 | 77.52 | 6890 | 19.33 | 75.5 |
| Existing **AHEG-FS** | 83.64 | 80.36 | 6390 | 16.35 | 70.3 |
| Proposed **NSPPS** | 86.16 | 83.54 | 5780 | 13.83 | 65.9 |
| Proposed **TSIDFE** | 88.82 | 85.25 | 5315 | 11.17 | 60.9 |
| **Proposed SCTPP-FS** | 90.79 | 87.14 | 4920 | 9.20 | 55.3 |

**Table 9.2 (b) Results of Feature Selection Techniques for Pneumonia dataset**

| Methods/Metrics | Training FA (%) | Testing FA (%) | Feature Selection time (ms) | Error rate (%) | Space complexity (KB) |
|---|---|---|---|---|---|
| Existing **Chi$^2$-MI** | 84.67 | 79.52 | 6090 | 15.32 | 71.25 |
| Existing **AHEG-FS** | 86.57 | 82.14 | 5480 | 13.42 | 68.59 |
| Proposed **NSPPS** | 88.72 | 85.62 | 3990 | 11.27 | 61.52 |
| Proposed **TSIDFE** | 91.10 | 87.63 | 3320 | 8.89 | 54.62 |
| **Proposed SCTPP-FS** | 93.9 | 89.25 | 3070 | 6.1 | 50.4 |

Table 9.2 (a) and (b) demonstrate the experimental results of feature selection accuracy, time, error rate, and space complexity for enhancing the performance of disease detection for COVID-19 as well as the Pneumonia dataset. The functionality of the proposed feature selection techniques, namely the NSPPS Model, TSIDFE Technique, and SCTPP-FS Technique, is compared with conventional AHEG-FS and Chi$^2$-MI. According to the table, the proposed NSPPS Model, TSIDFE Technique, and SCTPP-FS Technique achieve improved accuracy in selecting relevant feature data compared to existing methods. Specifically, the proposed SCTPP-FS Technique achieved higher feature selection accuracy than the other proposed methods.

Different ranges of patient data samples are selected from the given database to perform the feature selection process. By observing the above table, the feature selection accuracy of the proposed SCTPP-FS technique is higher than other proposed and conventional techniques.

The higher accuracy of feature selection using the SCTPP-FS technique is attained by means of applying Kaiser–Meyer–Olkin correlative projection pursuit. With this, the association between two features is measured. According to the correlation measure, the input features are categorized as relevant and irrelevant. By identifying the two different sets of features, relevant features for predicting the disease are selected with more accuracy. This, in turn, results in higher feature selection accuracy being achieved in the SCTPP-FS technique than in other techniques. The average outcome of feature selection accuracy for the SCTPP-FS technique is enhanced by 9% and 13% compared to the existing AHEG-FS and Chi$^2$-MI methods, respectively, for the

COVID-19 dataset. Additionally, the results depicts that the feature selection accuracy using the TSIDFE method increases by 8% and 11% compared to the AHEG-FS and $Chi^2$-MI methods, respectively, for the Pneumonia dataset, which is calculated by differentiating the existing and proposed percentage and divide the same by existing percentage and multiply the answer by hundred.

In addition, the proposed SCTPP-FS Technique performs relatively well, yielding better results in less time while selecting pertinent features of patient data samples compared to other proposed and conventional techniques. Through the application of statistical correlative targeted projection pursuit, the proposed SCTPP-FS technique carried out feature selection with minimum time to detect the performance of disease detection. The features from the dataset are gathered, and the Kaiser–Meyer–Olkin correlation is computed between the features. With this correlation measure, highly and lowly correlated aspects are identified as of database. Higher correlated aspects are identified as more informative features for disease detection. By selecting the most relevant aspects from the database, model performance and effectiveness are improved. By focusing solely on the most informative features, feature selection can significantly reduce the model's complexity. A less complex model generally requires less time for both training and prediction because it has fewer calculations to perform. In other words, a less complex model makes predictions faster because they avoid unnecessary computations related to irrelevant features. Therefore, less time is achieved in the proposed technique. For COVID-19, the average outcome of feature selection time using the SCTPP-FS technique is reduced by 23% and 29% contrasted to the existing AHEG-FS and $Chi^2$-MI methods, respectively. Additionally, the results feature selection time using the TSIDFE method is minimized by 17% and 23% compared to the AHEG-FS and $Chi^2$-MI methods, respectively. In addition, the proposed NSPPS Model minimizes the average feature selection time by 10% and 16% compared to the AHEG-FS and $Chi^2$-MI methods.

The compared values clearly demonstrate that the SC of the SCTPP-FS method is the minimum compared to the other feature selection methods. The minimum space complexity is attained by applying the Kaiser–Meyer–Olkin correlative projection pursuit in the SCTPP-FS technique. The designed projection method is a type of dimensionality reduction technique used

to compute correlations among aspects and select pertinent features from the given dataset. The maximum correlated features are selected as relevant. Additionally, the minimum correlated features are removed to reduce the dataset's dimensionality. This, in turn, decreases the space complexity of the SCTPP-FS technique compared to other methods. The experimental results show that the space complexity of the proposed SCTPP-FS technique is reduced by 27% and 21% compared to the conventional AHEG-FS and $Chi^2$-MI methods, respectively, for the COVID-19 dataset. The output space complexity using the TSIDFE method is decreased by 13% and 19% compared to the AHEG-FS and $Chi^2$-MI methods, respectively. Additionally, the space complexity results for the proposed NSPPS Model were minimized by 6% and 13% compared to the AHEG-FS and $Chi^2$-MI techniques.

The outcomes of ER with the SCTPP-FS technique are decreased by 44% and 39% compared to the conventional AHEG-FS and $Chi^2$-MI methods, respectively. The outcome of the error rate using the TSIDFE method is reduced by 33% and 42% compared to the AHEG-FS and $Chi^2$-MI methods, respectively. Additionally, the error rate output using the proposed NSPPS Model was reduced by 15% and 28% compared to the existing AHEG-FS and $Chi^2$-MI methods, respectively.

The feature selection time is minimised by 44%, 50% using the proposed SCTPP-FS Technique compared to existing AHEG-FS and $Chi^2$-MI, respectively, for the Pneumonia dataset. The error rate is cut down by 34% and 42% using the proposed TSIDFE technique compared to the existing AHEG-FS and $Chi^2$-MI, respectively, for the Pneumonia dataset. Additionally, the space complexity of the SCTPP-FS technique is lowered by 27% and 29% compared to existing AHEG-FS and $Chi^2$-MI, respectively, for the Pneumonia dataset.

### 9.3.5 Performance of ROC Curve for feature selection

True positives and false positives are used to measure the ROC curve. By using the ROC curve, feature selection is performed to identify correctly predicted and incorrectly predicted instances.

**Table 9.2 (c) Tabulation for ROC Curve for feature selection**

| False Positive Rate | True Positive Rate | | | | |
|---|---|---|---|---|---|
| | Existing $Chi^2$-MI | Existing AHEG-FS | Proposed NSPPS | Proposed TSIDFE | Proposed SCTPP-FS |
| 0.1 | 0 | 0 | 0 | 0 | 0 |
| 0.2 | 0.25 | 0.27 | 0.3 | 0.33 | 0.37 |
| 0.3 | 0.3 | 0.34 | 0.4 | 0.43 | 0.48 |
| 0.4 | 0.38 | 0.43 | 0.46 | 0.5 | 0.54 |
| 0.5 | 0.46 | 0.49 | 0.53 | 0.58 | 0.61 |
| 0.6 | 0.55 | 0.59 | 0.62 | 0.65 | 0.69 |
| 0.7 | 0.61 | 0.64 | 0.66 | 0.68 | 0.73 |
| 0.8 | 0.66 | 0.69 | 0.71 | 0.74 | 0.79 |
| 0.9 | 0.7 | 0.72 | 0.75 | 0.79 | 0.82 |
| 1 | 0.76 | 0.79 | 0.84 | 0.86 | 0.9 |

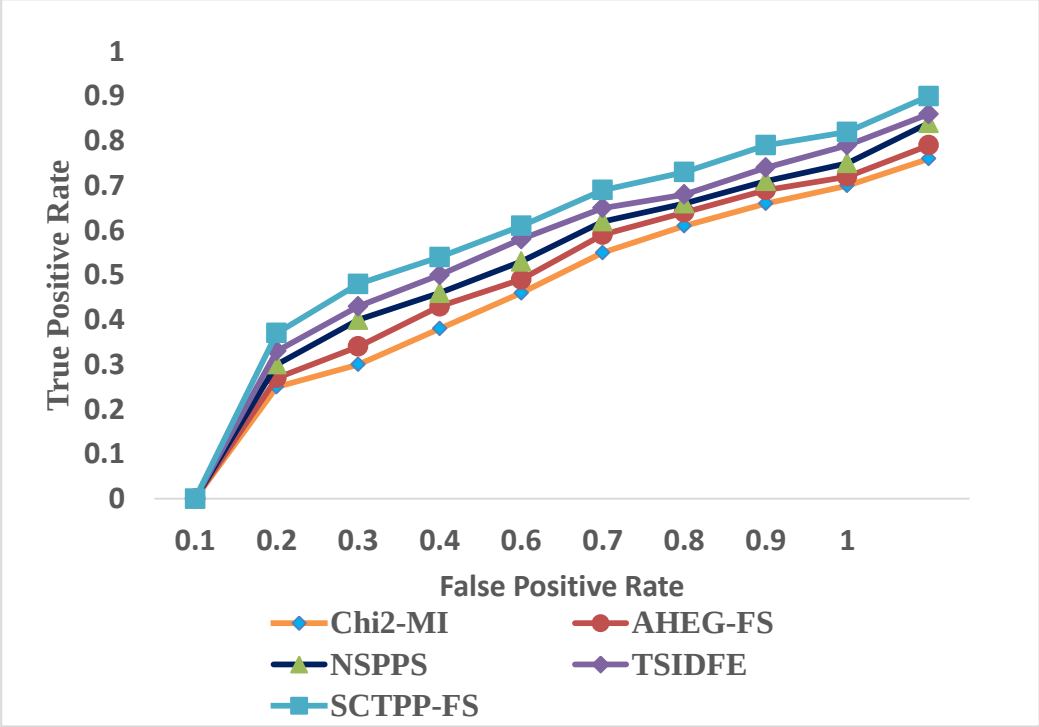


**Figure 9.2 Results of ROC Curve for feature selection**

Figure 9.2 visualise the outcome of the ROC curve analysis of the proposed NSPPS Model, TSIDFE Technique, and SCTPP-FS Technique, which are compared with existing AHEG-FS and Chi$^2$-MI methods. From Figure 9.2, it is prooved that the ROC curve of the SCTPP-FS Technique is comparatively enhanced compared to existing methods.

## 9.4 RESULTS AND DISCUSSION FOR CLASSIFICATION

Outcomes of the proposed EPBC technique, TCLMCNL technique, and MO-UNetDL technique are compared with existing methods, LSTM ensemble model and DSPM.

### 9.4.1 Results of Prediction Accuracy

It is designated as the proportion of patient data samples exactly forecasted as normal or disease cases during classification to the overall patient data. It is also known as classification accuracy and is mathematically calculated, as shown below.

$$\mathrm{PAC} = \left[\frac{\mathrm{tp+tn}}{\mathrm{tp+tn+f_p+f_n}}\right] * 100 \qquad (9.9)$$

Where '$PAC$' symbolizes the prediction accuracy, '$tp$' refers true positive, '$tn$' symbolizes true negative, '$fp$' symbolizes false positive, '$fn$' denotes false negative. The accuracy metric is calculated in percentage (%).

### 9.4.2 Impact of Precision

Precision is computed depending on true positives and false negatives. It is computed as follows.

$$\mathrm{Pre} = \left(\frac{\mathrm{tp}}{\mathrm{tp+f_p}}\right) * 100 \qquad (9.10)$$

Where '$Pre$' refers a Precision, '$tp$' refers true positive, '$f_p$' refers false positive. It is estimated in percentage (%).

### 9.4.3 Performance of Recall

Recall is computed depending on the measure of as well as of disease prediction. It is also referred to as sensitivity, and it is computed as follows.

$$Rec = \left(\frac{tp}{tp+fn}\right) * 100 \qquad (9.11)$$

Where '$Rec$' refers a recall, '$tp$' refers true positive, '$fn$' denotes false negative. Recall is calculated in percentage (%).

### 9.4.4 Study of Specificity

Specificity is determined on the basis of true negatives and false positives of disease forecast. It is mathematically estimated as given below,

$$Spec = \left(\frac{tn}{tn+fp}\right) * 100 \quad (9.12)$$

Where '$Spec$' refers specificity, '$tn$' refers the true negative, '$fp$' refers the false positive. The specificity is computed in percentage (%).

### 9.4.5 Analysis of Prediction time

Prediction time or classification time is calculated as the timespan required by the method to forecast whether a patient is influenced by a disease or not through the classification process. It is given below.

$$PTime = \sum_{i=1}^{n} P_i * Time\,[PSP] \quad (9.13)$$

Where '$PTime$' is a prediction time, '$P_i$' is a patients involved in simulation '$Time\,[PSP]$' is time taken to classify solitary patient data sample. It is calculated in milliseconds (ms).

**Table 9.3 (a) Results of Classification Techniques for COVID-19 dataset**

| Methods/Metrics | Training CA (%) | Testing CA (%) | Prediction Time (ms) | Precision (%) | Recall (%) | Specificity (%) |
|---|---|---|---|---|---|---|
| Existing Deep learning LSTM ensemble model | 94.14 | 90.25 | 6760 | 94.51 | 95.64 | 45.87 |
| Existing DSPM | 95.13 | 91.16 | 6270 | 95.86 | 96.79 | 47.28 |
| Proposed EPBC | 96.18 | 92.65 | 5640 | 97.07 | 97.60 | 50.52 |
| Proposed TCLMCNL | 96.83 | 93.52 | 5210 | 97.95 | 98.52 | 52.89 |
| Proposed MO-UNetDL | **97.90** | **94.25** | **4740** | **98.86** | **99.15** | **56.56** |

**Table 9.3 (b) Results of Classification Techniques for Pneumonia dataset**

| Methods/Metrics | Training CA (%) | Testing CA (%) | Prediction Time (ms) | Precision (%) | Recall (%) | Specificity (%) |
|---|---|---|---|---|---|---|
| Existing Deep learning LSTM ensemble model | 94.26 | 91.24 | 4021 | 93.01 | 91.23 | 48.63 |
| Existing DSPM | 96.15 | 92.14 | 3850 | 94.01 | 92.46 | 50.24 |
| Proposed EPBC | 97.5 | 93.54 | 3425 | 94.25 | 93.41 | 53.63 |
| Proposed TCLMCNL | 97.1 | 94.25 | 3010 | 95.38 | 95.69 | 55.25 |
| Proposed MO-UNetDL | 98 | 96.24 | 2056 | 98.46 | 97.65 | 59.25 |

Table 9.3(a) and (b) depicts the comparative evaluation of the disease prediction accuracy, time, precision, recall, and specificity for the proposed EPBC technique, TCLMCNL technique, and MO-UNetDL technique with existing deep learning LSTM ensemble model and DSPM for COVID-19 and Pneumonia dataset. According to the table, the proposed EPBC technique, TCLMCNL technique, and MO-UNetDL technique yield better results than the conventional DL LSTM ensemble method and DSPM, respectively.

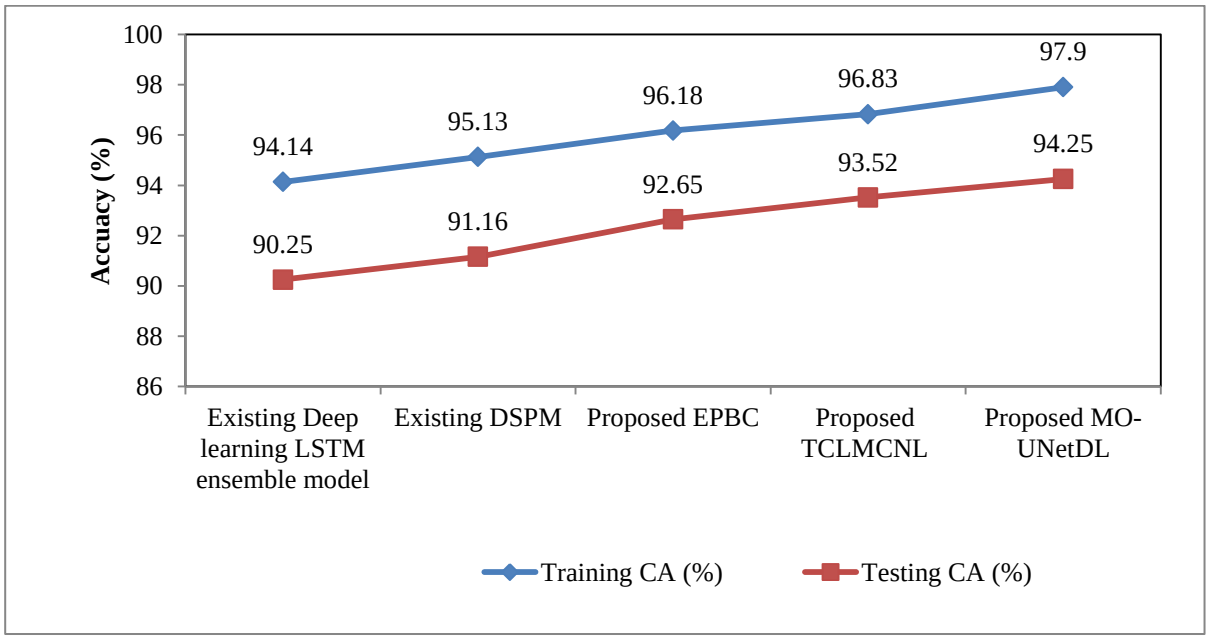


**Figure 9.3 (a) Results of Classification accuracy for COVID-19 dataset**

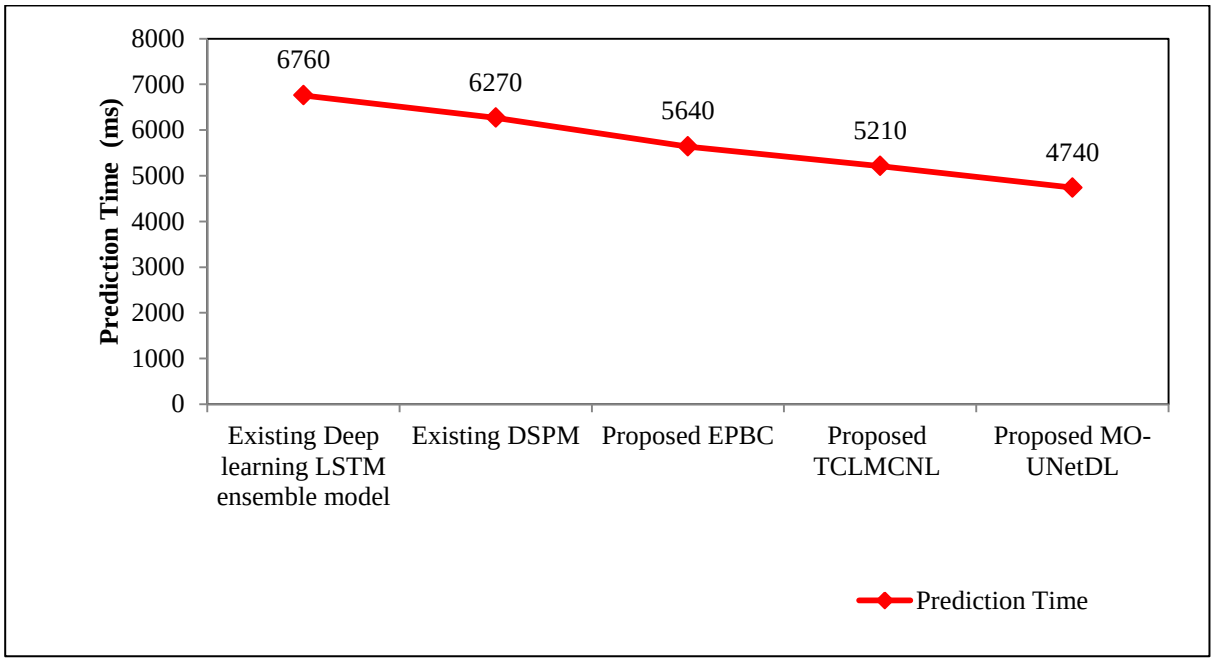


**Figure 9.3 (b) Results of Prediction Time for COVID-19 dataset**

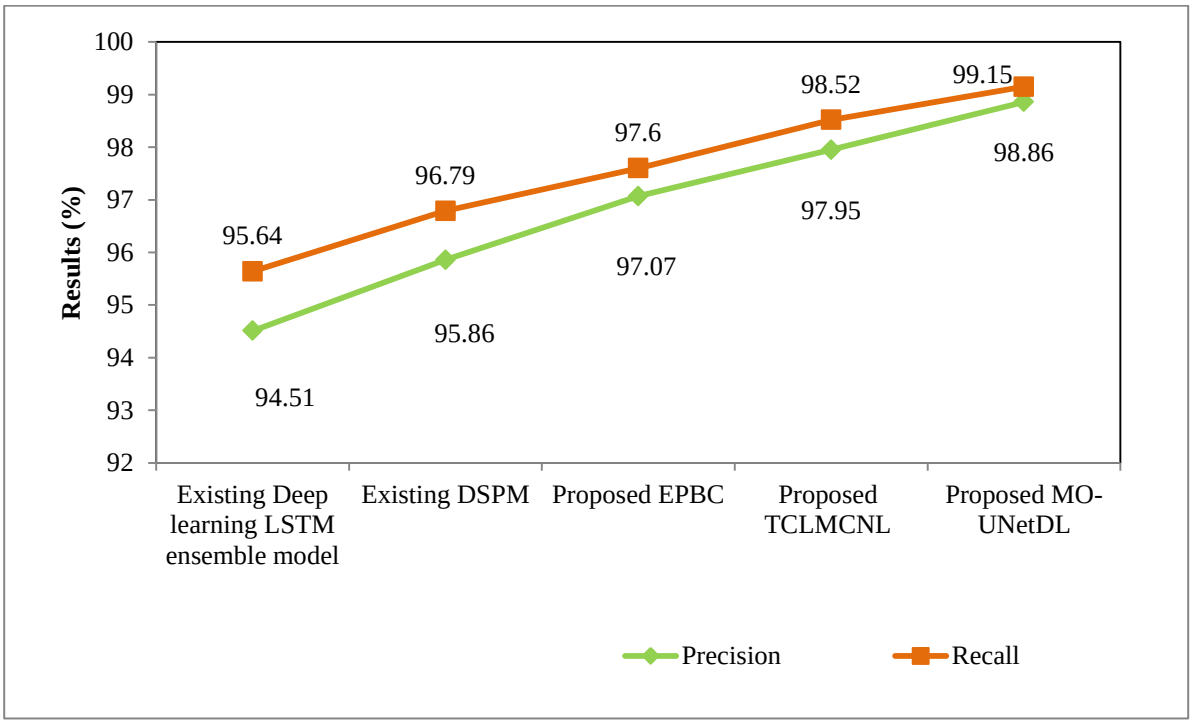


**Figure 9.3 (c) Results of Precision and Recall for COVID-19 dataset**

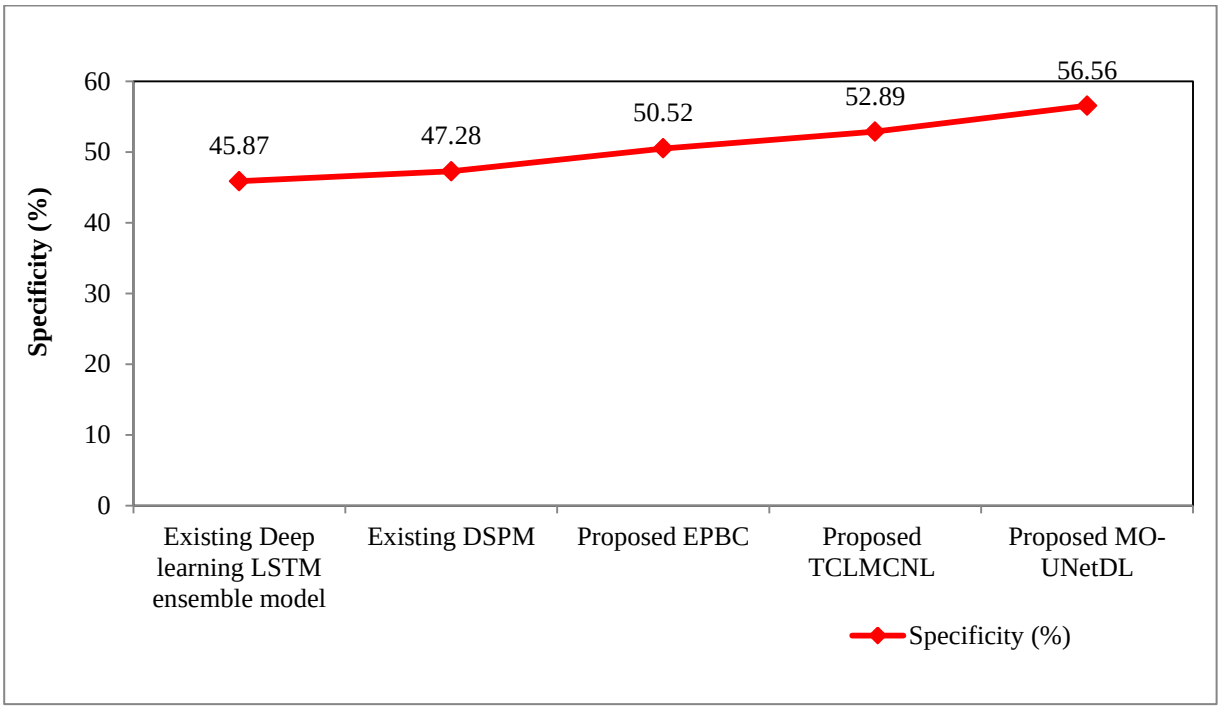


**Figure 9.3 (d) Results of Specificity for COVID-19 dataset**

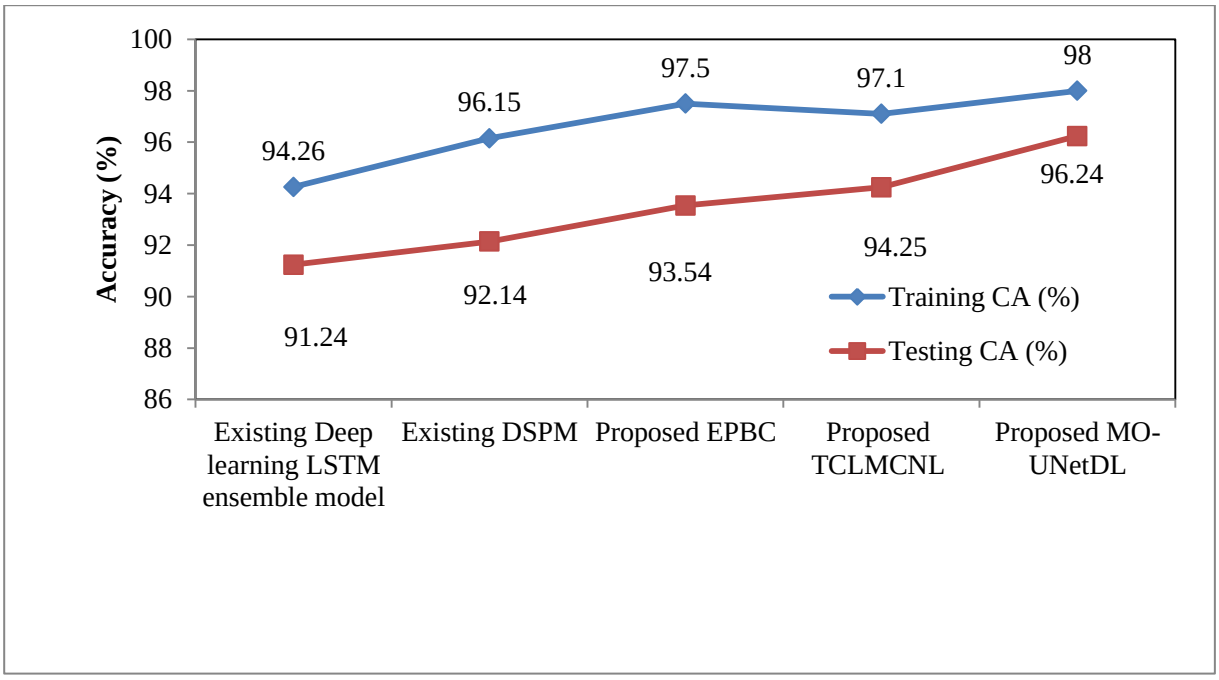


**Figure 9.3 (e) Results of Classification Accuracy for Pneumonia dataset**

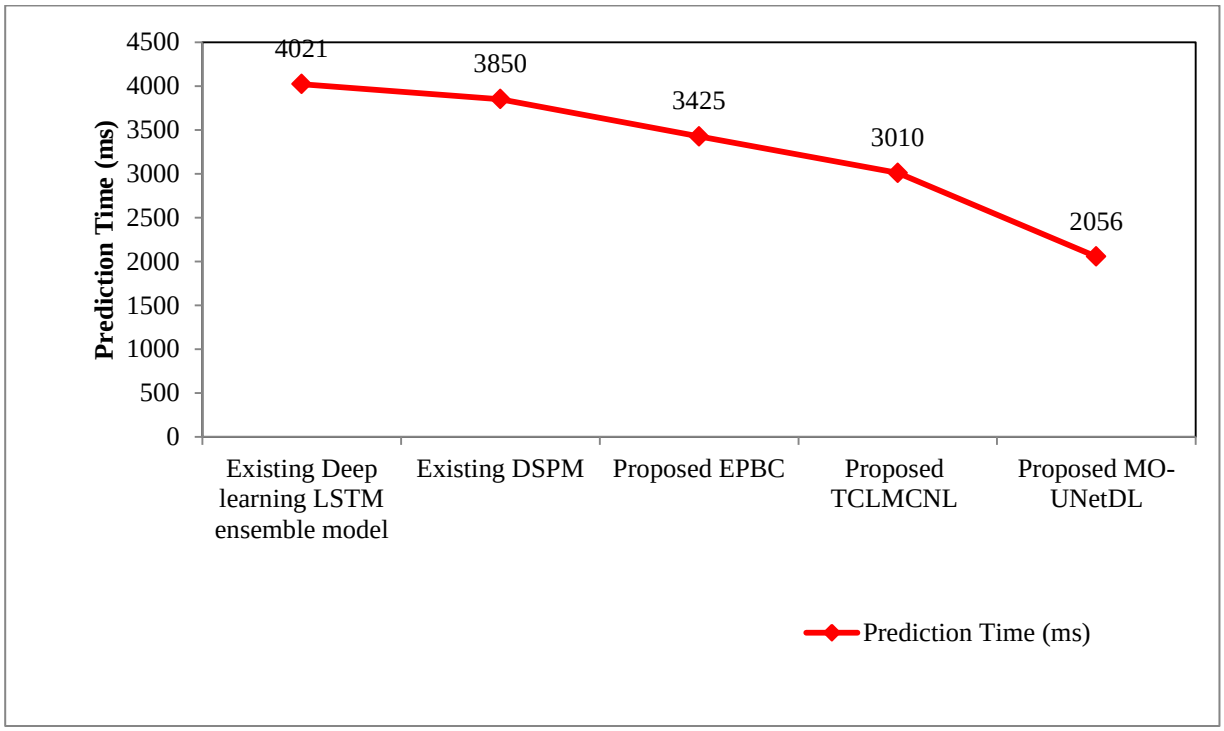


**Figure 9.3 (f) Results of Prediction Time for Pneumonia Dataset**

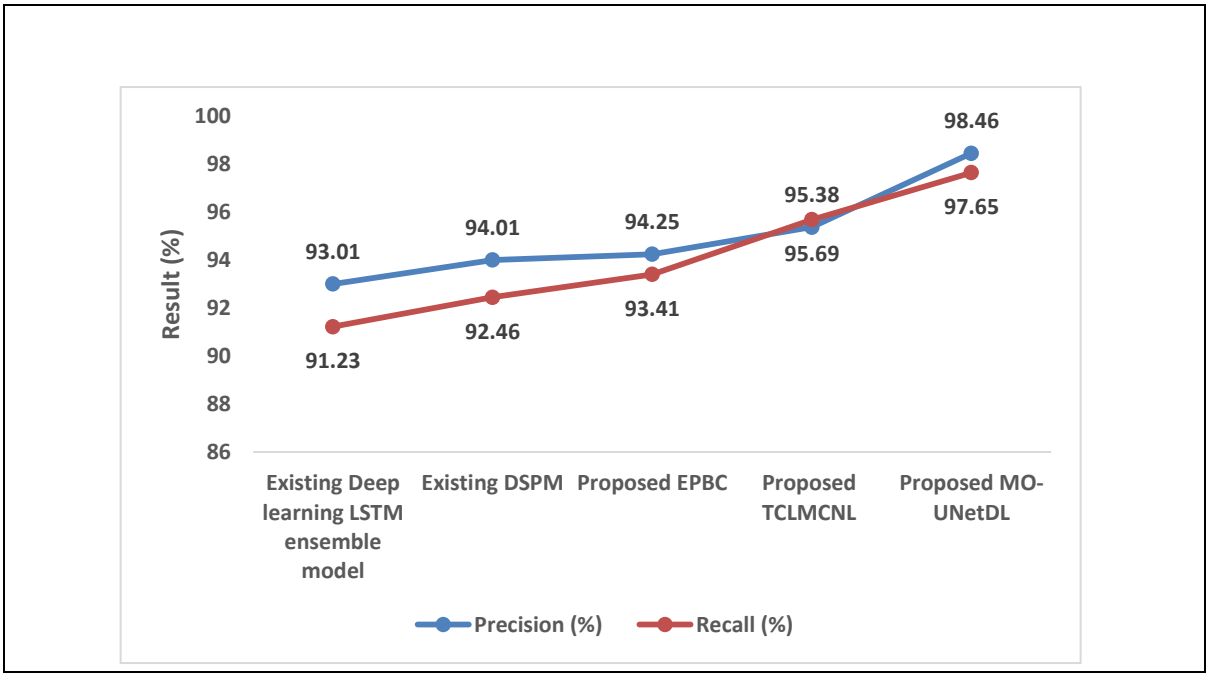


**Figure 9.3 (g) Results of Precision and Recall for Pneumonia Dataset**

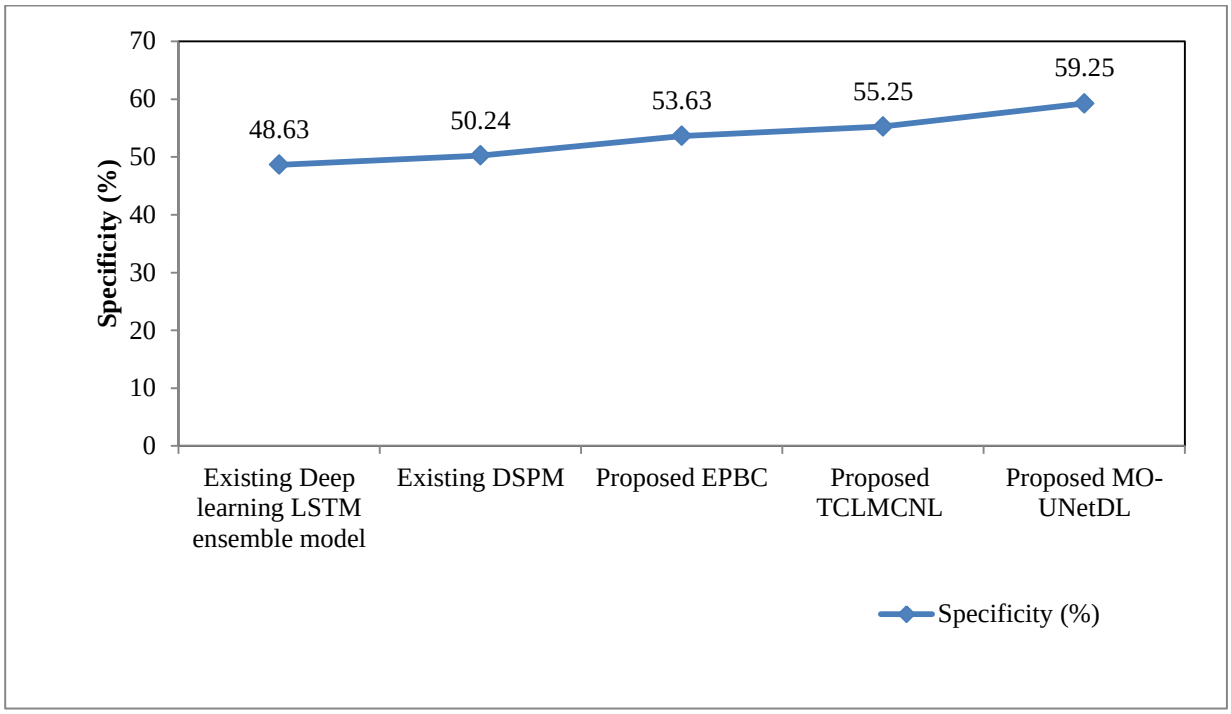


**Figure 9.3 (h) Results of Specificity for Pneumonia dataset**

Figures 9.3 (a) to 9.3 (h) depict a graphical illustration of disease prediction time, precision, specificity, and recall for different classification methods using two datasets COVID-19 and Pneumonia. The performance of accuracy using the proposed EPBC technique, TCLMCNL technique, and MO-UNetDL techniques are compared with that of the available deep learning LSTM ensemble model and DSPM. According to the results, it is evident that the MO-UNetDL method significantly enhances accuracy related to other methods. This is because of the application of a memetic-optimized U-Net deep learning classifier. In this classifier, Wilcox's index coefficient is computed to examine the testing, training data samples. Additionally, the soft step activation function is employed to evaluate the coefficient results and yields the final classification outcomes. According to the classification results, the disease and normal data are accurately predicted. Thus, the outcome of disease prediction accuracy using the proposed MO-UNetDL technique (was evaluated using Equation 3.12) improve by 4% and 3% compared to the deep learning LSTM ensemble model and DSPM for the COVID-19 database. Additionally, the disease prediction accuracy of the proposed MO-UNetDL technique is improved by 2% and 4% compared to the deep learning LSTM ensemble model and DSPM for

the pneumonia database. The mean of ten comparison outcomes indicates that the precision of the proposed MO-UNetDL method is improved by 4% and 3% compared to the deep learning LSTM ensemble model and DSPM, respectively for COVID – 19 dataset. Also, mean of ten comparison outcomes illustrates that the recall of the proposed MO-UNetDL method is increased by 4% and 2% compared to the deep learning LSTM ensemble method and DSPM. The performance of specificity in COVID-19 dataset, using the proposed MO-UNetDL technique is enhanced by 23% and 20% compared to the deep learning LSTM ensemble model and DSPM. In COVID-19 dataset the execution outcomes of the prediction time of the MO-UNetDL method are significantly minimized by 30% and 24% compared to the deep learning LSTM ensemble model and DSPM.

### 9.4.6 Examination of Kappa statistics

Kappa statistics is a parameter to compute an experimental accuracy with a probable accuracy.

$$\text{Ks} = \frac{O(A)-P(A)}{(1-P(A))} \tag{9.14}$$

Where '$O(A)$' denotes the observed accuracy and '$P(A)$' denotes the proportion of probable accuracy by chance. The value of Kappa statistics is ranged between '0' and '1'. The value of the Kappa statistic nearer to 1 refers the better performance of the method.

**Table 9.4 Kappa Statistics**

| Methods | Kappa Statistics |
|---|---|
| **EPBC** | **0.85** |
| **TCLMCNL** | **0.87** |
| **MO-UNet DL** | **0.9** |
| **Deep-LSTM Ensemble Model** | **0.79** |
| **DSPM** | **0.82** |

Table 9.4 illustrates the measure of Kappa statistics for five various techniques, including EPBC, TCLMCNL, MO-UNetDL, the deep learning LSTM ensemble model, and DSPM.

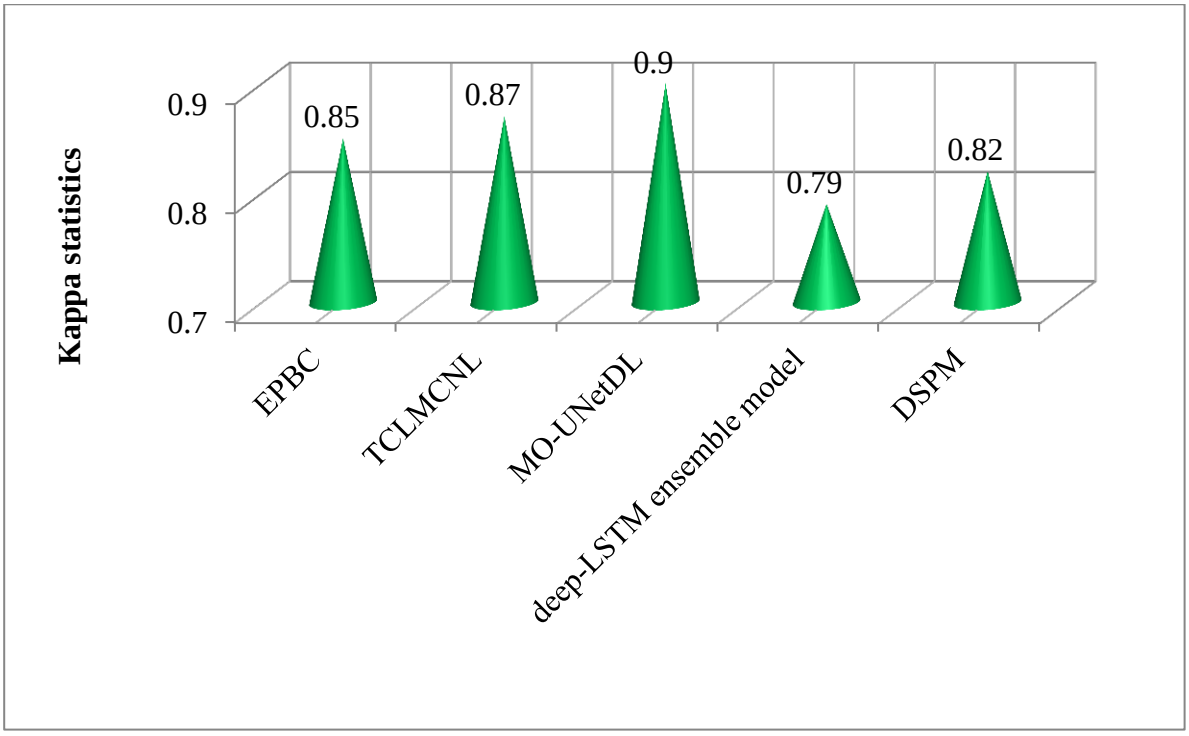


**Figure 9.3 (i) Results of Kappa Statistics**

Figure 9.3(i) shows a performance study of kappa statistics across the class for five different classification techniques. In the above graph, the x-axis denotes the five techniques, and the y-axis denotes the performance of kappa statistics for each method. As analyzed in the above Figure, the MO-UNetDL technique achieved 0.9, which is better than the EPBC, TCLMCNL, deep learning LSTM ensemble model, and DSPM. It is also clear that the MO-UNetDL technique obtains the better value of kappa statistics. The performance of kappa statistics using the MO-UNetDL method is improved by 14% and 10% than the conventional methods.

### 9.4.7 Investigation of Receiver Operating Characteristic (ROC)

The ROC curve is examined for computing the disease prediction rate performance. With the help of the ROC curve, classification is performed depending on correctly predicted or wrongly predicted outcomes. Depending on true positives and false positives, the ROC curve is evaluated.

**Table 9.5 Tabulation for ROC Curve**

| False Positive Rate | True Positive Rate | | | | |
|---|---|---|---|---|---|
| | **Existing Deep Learning LSTM ensemble Model** | **Existing DSPM** | **Proposed EPBC** | **Proposed TCLMCNL** | **Proposed MO-UNetDL** |
| 0.1 | 0 | 0 | 0 | 0 | 0 |
| 0.2 | 0.28 | 0.33 | 0.37 | 0.4 | 0.43 |
| 0.3 | 0.35 | 0.42 | 0.46 | 0.5 | 0.53 |
| 0.4 | 0.48 | 0.51 | 0.56 | 0.6 | 0.63 |
| 0.5 | 0.52 | 0.62 | 0.65 | 0.67 | 0.7 |
| 0.6 | 0.6 | 0.68 | 0.71 | 0.74 | 0.76 |
| 0.7 | 0.67 | 0.75 | 0.78 | 0.81 | 0.83 |
| 0.8 | 0.72 | 0.79 | 0.83 | 0.86 | 0.88 |
| 0.9 | 0.78 | 0.82 | 0.85 | 0.9 | 0.93 |
| 1 | 0.85 | 0.88 | 0.93 | 0.97 | 1 |

The ROC curve analysis values of the EPBC, TCLMCNL, and MO-UNetDL techniques using conventional methods are provided in Table 9.5. From the above table, the ROC curve of the proposed MO-UNetDL technique is found to be better than that of the other methods.

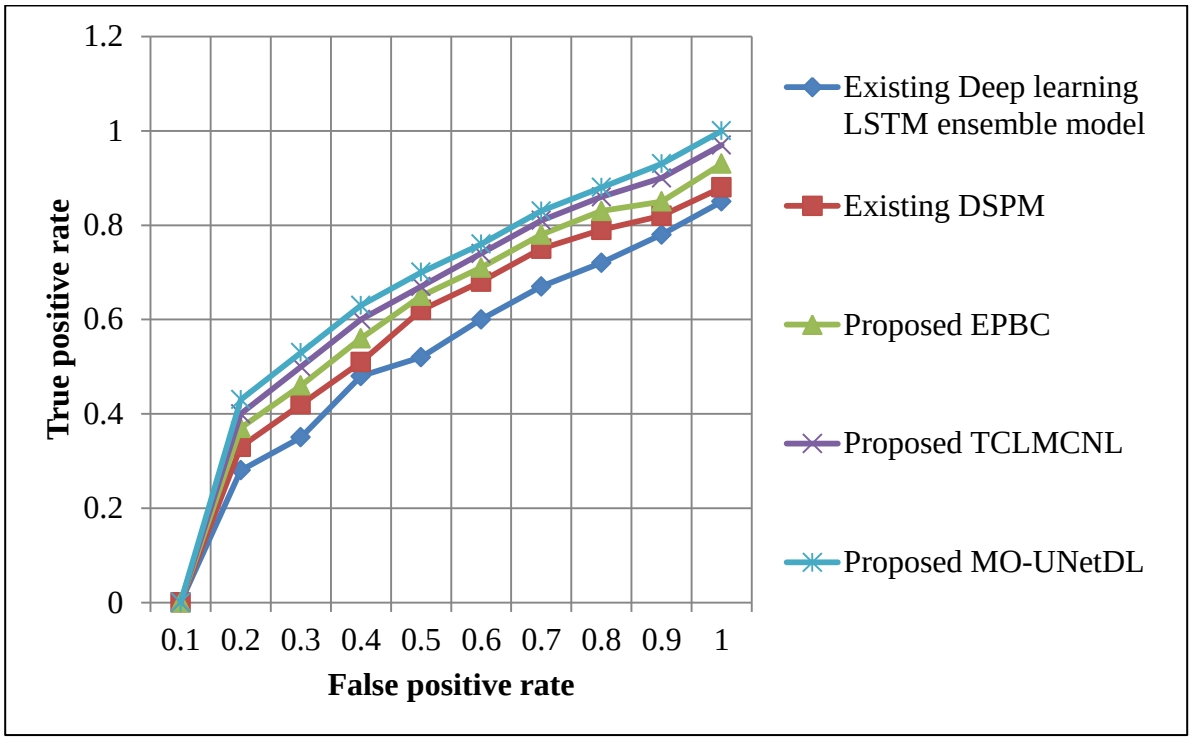


**Figure 9.3 (j) Results of ROC Curve**

Figure 9.3 (j) visualise a graphical illustration of the ROC curve analysis of the introduced EPBC, TCLMCNL, MO-UNetDL technique, deep learning LSTM ensemble model, and DSPM. In addition, ROC analyzes the disease prediction based on the true positive rate and false positive rate for every probable value. From the above Figure, it is illustrative that the ROC curve of the MO-UNetDL technique is comparatively enhanced compared to existing methods.

### 9.4.8 Results of Area Under the Curve (AUC)

AUC is a significant factor in the evaluation model. The output of the AUC is constantly varied in the range of values from 0 to 1. The AUC curve is plotted depending on true positive as well as true negative.

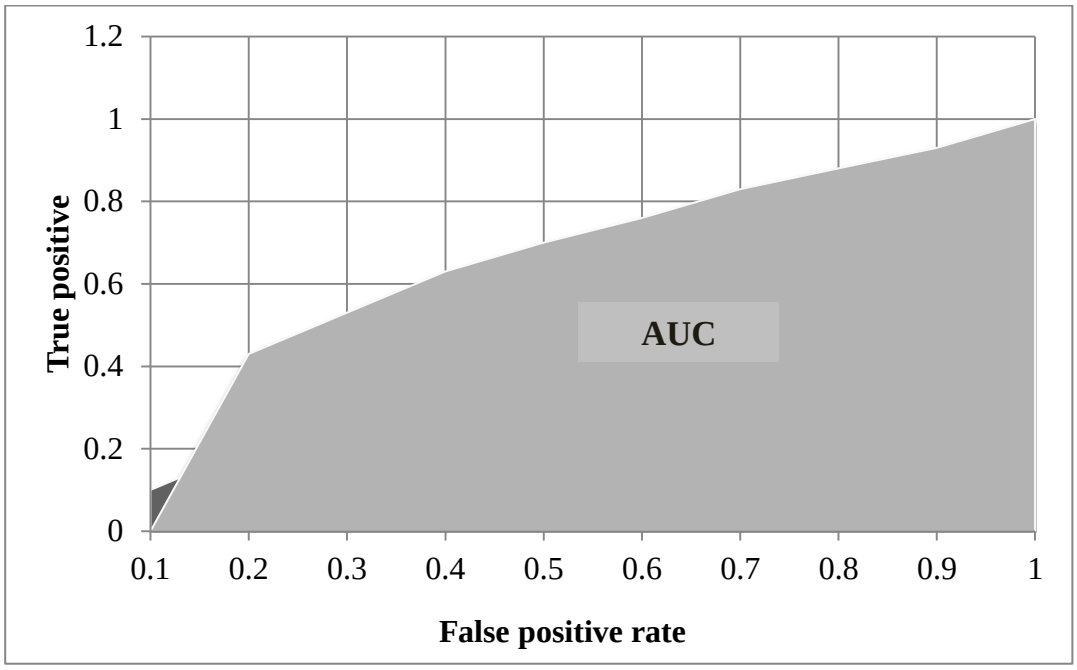


**Figure 9.3 (k) Results of AUC for MO-UNetDL Technique**

Figure 9.3 (k) describes the AUC curve for the proposed MO-UNetDL technique according to the true positive and false positive. The result of the MO-UNetDL classifier technique is better when the AUC score is higher. This indicates that the MO-UNetDL gives maximum prediction accuracy.

### 9.4.9 Statistical Test

In our work, the ANOVA test is used. ANOVA test is a statistical test used to analyze the distinction among the means of more than two groups. ANOVA test outcomes were employed in an F-test. The proposed EPBC, TCLMCNL, and MO-UNetDL techniques are employed to measure the ANOVA test, as depicted in Figure 9.3 (l).

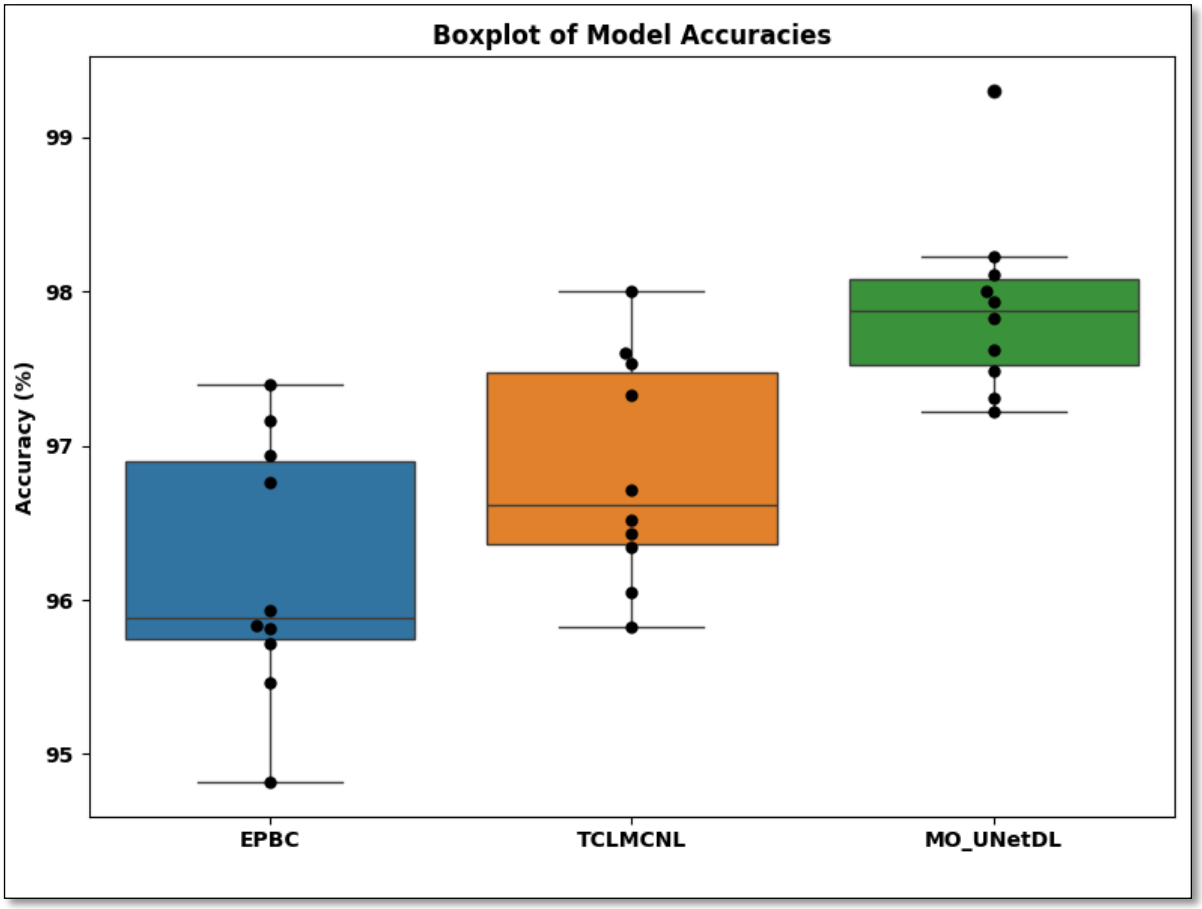


**Figure 9.3 (l) Results of ANOVA test for proposed EPBC, TCLMCNL and MO-UNetDL techniques**

Figure 9.3 (l) describes the ANOVA test for the three proposed techniques according to accuracy. Result of MO-UNetDL technique is better than other methods.

## 9.5 RESULTS AND DISCUSSION FOR COVID-19 AND RSNA PNEUMONIA DATASETS

Performance outcomes of proposed classification techniques, such as EPBC, TCLMCNL, and MO-UNetDL, are implemented in Python. The results of disease identification using the aforementioned techniques are examined utilising the COVID-19 Corona Virus India Dataset and the RSNA Pneumonia Recognition Challenge database. The COVID-19 database on Kaggle includes eight .csv files. Additionally, the COVID-19 dataset is also collected from https://github.com/CSSEGISandData/COVID-19.This database includes daily case reports, USA

daily state reports, and Time-series summaries. The daily case report includes attributes such as FIPS, Admin2, and others. The RSNA Pneumonia Detection Challenge dataset is used to detect pneumonia in medical images. The outcomes of the proposed classification techniques are compared with those of relevant conventional techniques using dissimilar performance parameters.

### 9.5.1 Comparative Results of Classification without Preprocessing and Feature Selection Methods

In this sector, the performance of classification techniques, such as EPBC, TCLMCNL, and MO-UNetDL, is compared with that of an existing Deep learning LSTM ensemble model and DSPM without employing preprocessing and feature selection methods.

**Table 9.6 Classification without Preprocessing and Feature Selection**

| Classification Methods | COVID-19 Dataset | | | Pneumonia Dataset | | |
|---|---|---|---|---|---|---|
| | Accuracy (%) | Precision (%) | Recall (%) | Accuracy (%) | Precision (%) | Recall (%) |
| **Existing Deep Learning LSTM ensemble model** | 68.61 | 68.37 | 68.28 | 71.77 | 73.63 | 71.67 |
| **Existing DSPM** | 72.36 | 71.01 | 71.18 | 73.7 | 75.83 | 74.13 |
| **Proposed EPBC** | 74.37 | 73.18 | 72.92 | 75.64 | 77.79 | 76.81 |
| **Proposed TCLMCNL** | 76.76 | 75.49 | 74.48 | 78.68 | 79.82 | 78.79 |
| **Proposed MO-UNetDL** | 80.32 | 77.54 | 76.75 | 84.4 | 81.8 | 81.08 |

Table 9.6 shows the performance analysis of five classification methods without preprocessing and feature selection processes using the COVID-19 dataset and Pneumonia database. To validate the efficiency of the classification technique, the performance of accuracy, precision, and recall using the proposed EPBC, TCLMCNL, and MO-UNetDL is compared with that of the existing Deep Learning LSTM ensemble model and DSPM. From the results, the proposed MO-UNetDL method comparatively yields better results without preprocessing and feature selection processes than the other methods.

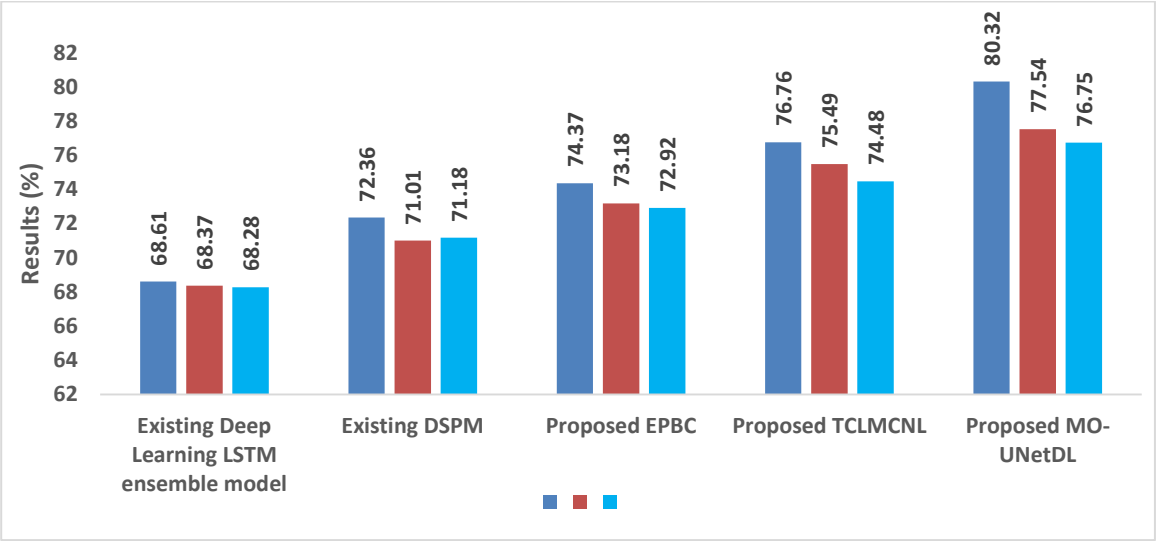


**Figure 9.4 (a) Results of Classification Accuracy without Preprocessing and Feature Selection for COVID - 19 Dataset**

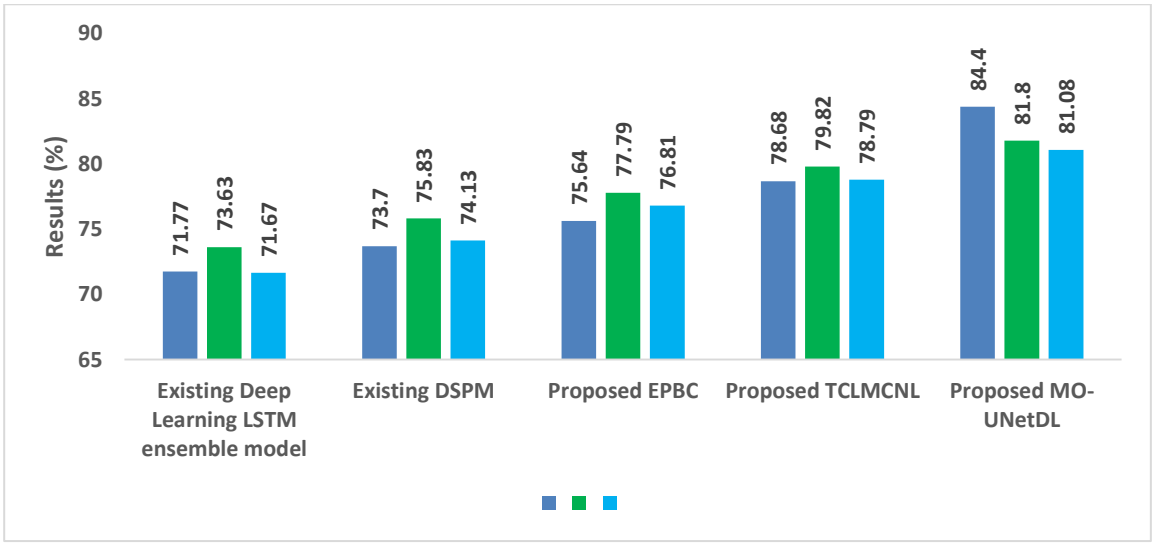


**Figure 9.4 (b) Results of Classification Accuracy without Preprocessing and Feature Selection for Pneumonia Dataset**

Figure 9.4 (a) and (b) illustrate the result of classification in accuracy, precision, recall metrics without preprocessing, and feature selection (w/o PP and FS) using two disease detection datasets. Through patient data gathered from input datasets, direct classification methods such as EPBC, TCLMCNL, and MO-UNetDL, along with the Deep Learning LSTM ensemble model and DSPM, are applied to classify the data and identify the disease in the patient. Before the classification, preprocessing and feature selection processes are not carried out. This leads to a

degradation of the classification results. However, the MO-UNetDL achieved comparatively higher results in accuracy, precision, and recall. This is due to the application of a memetic-optimized U-Net deep learning classifier. The accuracy of MO-UNetDL is improved by 11% and 14% for the datasets COVID-19 and Pneumonia respectively, compared to conventional methods. Additionally, the precision of MO-UNetDL increased by 9% and 8%, and the recall of MO-UNetDL increased by 8% and 9% for the two datasets.

### 9.5.2 Comparative Outcomes of Classification with Preprocessing without Feature Selection Methods

The performance of classification methods, with preprocessing (ZMFNE) and without feature selection, is analysed as follows.

**Table 9.7 Classification with Preprocessing (ZMFNE) without Feature Selection Methods**

| Classification Methods | COVID-19 Dataset | | | Pneumonia Dataset | | |
|---|---|---|---|---|---|---|
| | Accuracy (%) | Precision (%) | Recall (%) | Accuracy (%) | Precision (%) | Recall (%) |
| **Existing Deep Learning Ensemble Model** | 65.47 | 68.97 | 66.1 | 74.94 | 73.86 | 72.63 |
| **Existing DSPM** | 66.82 | 71.36 | 68.34 | 76.54 | 76.05 | 74.8 |
| **Proposed EPBC** | 71.23 | 73.6 | 73.29 | 78.83 | 78.99 | 76.61 |
| **Proposed TCLMCNL** | 75.87 | 75.48 | 75.32 | 81.19 | 81.01 | 79.02 |
| **Proposed MO-UNetDL** | 81.03 | 78.54 | 77.66 | 84 | 83.31 | 82.41 |

Table 9.7 presents the outcome of accuracy, precision, and recall of classification methods with preprocessing methods, excluding feature selection methods, for the datasets COVID-19 and Pneumonia. A comparative analysis of the proposed three methods is performed, as compared to the two conventional methods. As illustrated in the above table, the interpretation of classification using MO-UNetDL is improved in both datasets compared to other methods.

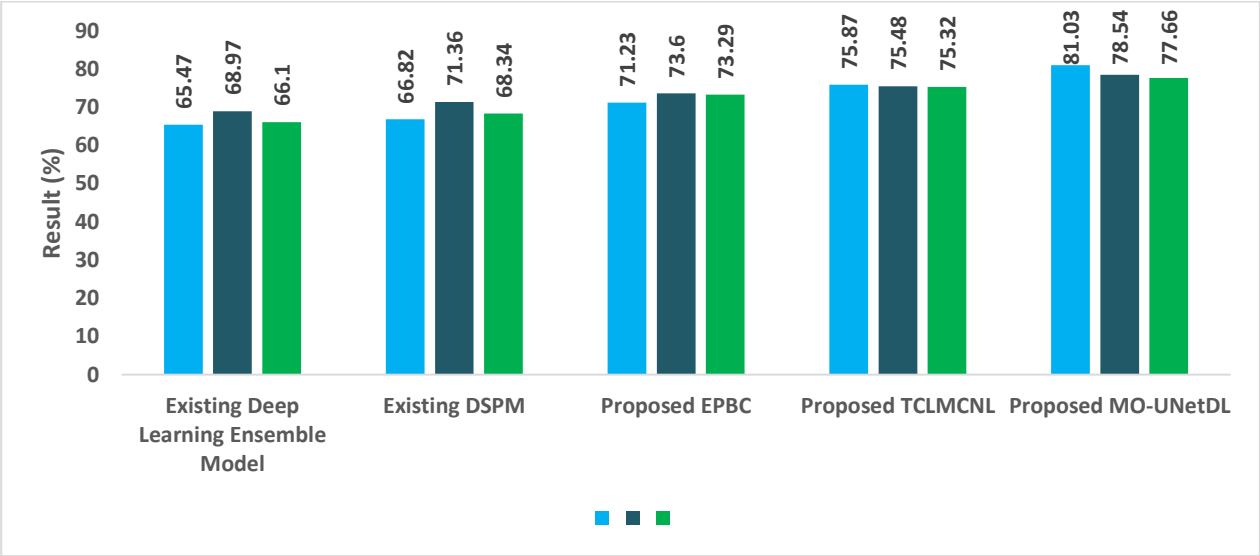


**Figure 9.5(a) Results of Classification Accuracy with Preprocessing without Feature Selection for COVID dataset**

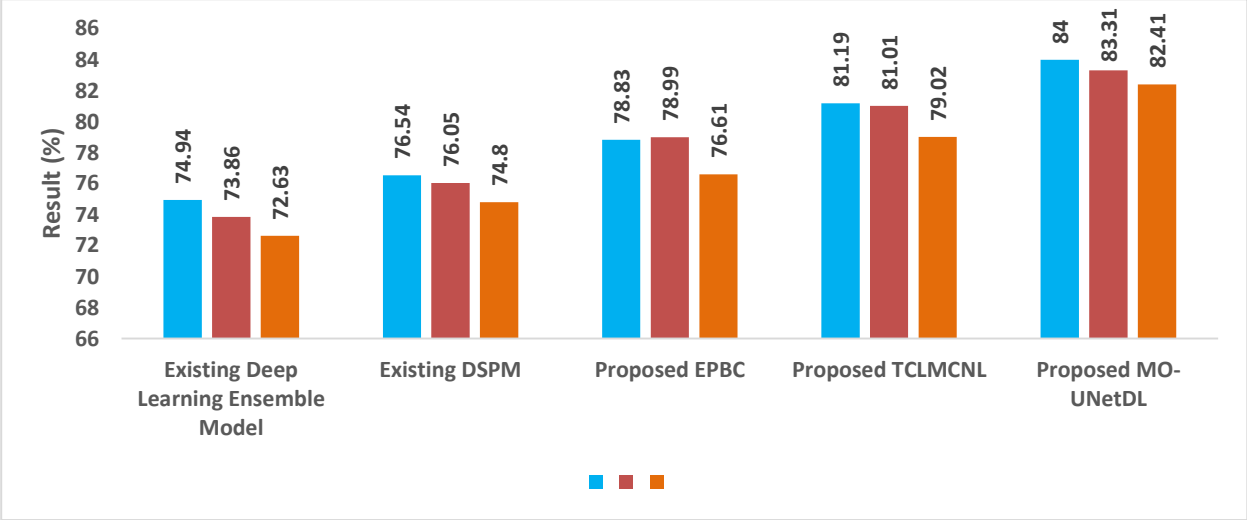


**Figure 9.5(b) Results of Classification Accuracy with Preprocessing and without Feature Selection for Pneumonia dataset**

Figures 9.5 (a) and (b) show the result of classification with a preprocessing process without feature selection using five different classification methods for two different datasets. As observed from the above figures, the results of classification using the proposed MO-UNetDL method are superior to those of the other methods in both datasets. In MO-UNetDL, a memetic-optimized U-Net deep learning classifier is applied to the preprocessing dataset to accurately identify patient data associated with the disease. With this, classification performance is

improved in MO-UNetDL. The accuracy of MO-UNetDL is increased by 21% and 10% compared to the existing methods for the datasets COVID-19 and Pneumonia respectively. Additionally, the precision of MO-UNetDL is enhanced by 10%, and the recall is increased by 14% and 10% for the COVID-19 dataset and the Pneumonia dataset, respectively.

### 9.5.3 Comparative Outcomes of Classification without Preprocessing with Feature Selection Methods

The performance of classification methods without preprocessing with feature selection (SCTPP) methods is compared in this section.

**Table 9.8 Classification without Preprocessing with Feature Selection (SCTPP_FS) Methods**

| Classification Methods | COVID-19 Dataset | | | Pneumonia Dataset | | |
|---|---|---|---|---|---|---|
| | Accuracy (%) | Precision (%) | Recall (%) | Accuracy (%) | Precision (%) | Recall (%) |
| **Existing Deep Learning Ensemble Model** | 67.26 | 70.95 | 68.72 | 77.27 | 76.74 | 75.56 |
| **Existing DSPM** | 71.02 | 74.74 | 71.75 | 78.92 | 78.04 | 78.76 |
| **Proposed EPBC** | 73.26 | 76.55 | 75.55 | 80.97 | 81.22 | 80.7 |
| **Proposed TCLMCNL** | 77.68 | 78.04 | 77.74 | 83.33 | 83.95 | 83.47 |
| **Proposed MO-UNetDL** | 83.53 | 81.4 | 80.98 | 87.04 | 86.58 | 85.46 |

Table 9.8 presents the classification results, including accuracy, precision, and recall, for the datasets COVID-19 and Pneumonia. Here, the performance of classification for disease prediction is analyzed in conjunction with a feature selection process. Compared to other classification methods, MO-UNetDL achieved better performance even without a preprocessing process.

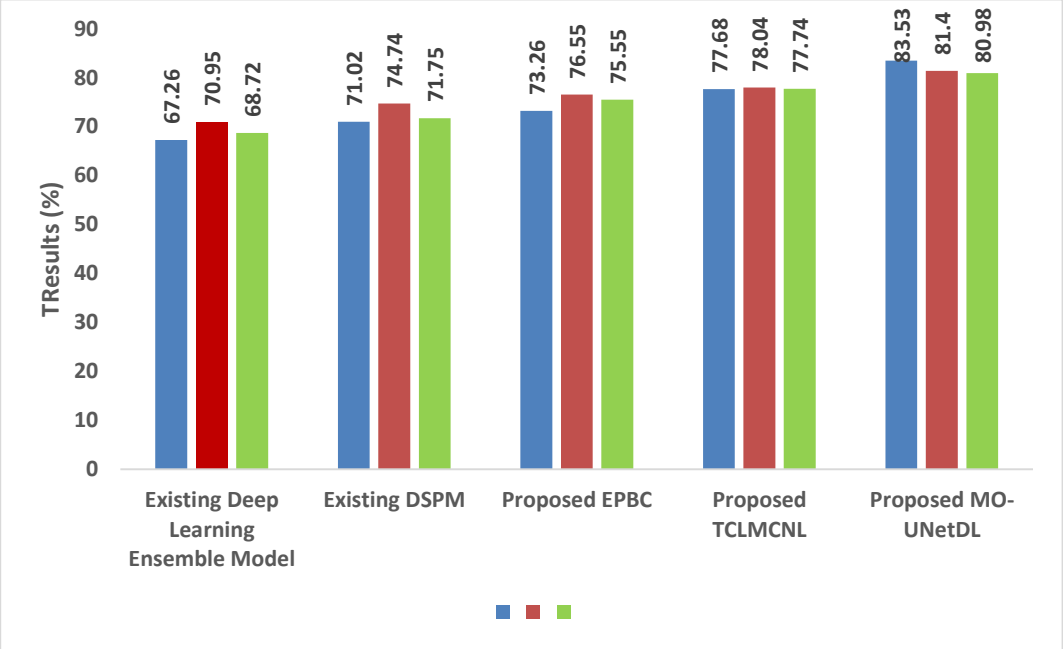


**Figure 9.5 (c) Outcomes of Classification without Preprocessing with Feature Selection for COVID-19 dataset**

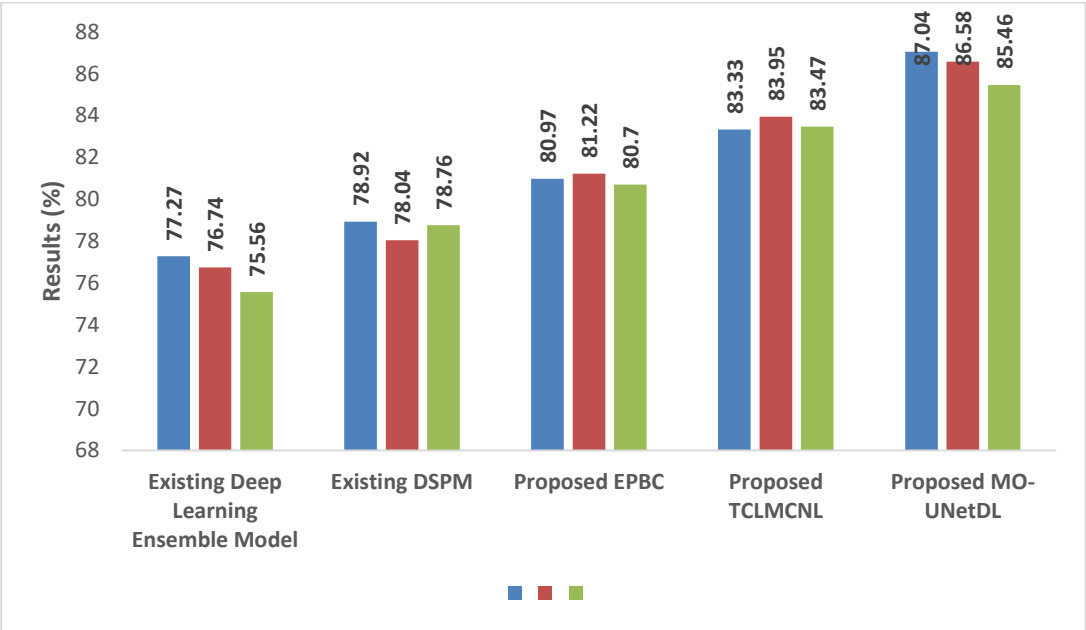


**Figure 9.5 (d) Outcomes of Classification without Preprocessing with Feature Selection for Pneumonia dataset**

Figure 9.5(c) and (d) depicts the classification performance of five methods without preprocessing with the feature selection process for the datasets COVID-19 and pneumonia. The

above figures clearly show that the MO-UNetDL method comparatively achieved better performance than other techniques. This is because the feature selection process selects only relevant aspects. Through carefully chosen features, classification is carried out accurately compared to other methods. The accuracy of classification using the proposed MO-UNetDL method is enhanced by 17% and 11% compared to existing methods for the datasets COVID-19 Pneumonia respectively. In addition, MO-UNetDL increases precision by 9% and 11% and recall by 13% and 9% for the datasets COVID-19 and Pneumonia respectively.

### 9.5.4 Comparative Results of Classification with Preprocessing and Feature Selection Methods

Classification outcomes of proposed as well as existing methods with preprocessing (ZMFNE) and feature selection (SCTPP) techniques is examined in this section.

**Table 9.9 Classification with Preprocessing (ZMFNE) and Feature Selection (SCTPP_FS)**

| Classification Methods | COVID-19 Dataset | | | Pneumonia Dataset | | |
|---|---|---|---|---|---|---|
| | Accuracy (%) | Precision (%) | Recall (%) | Accuracy (%) | Precision (%) | Recall (%) |
| **Existing Deep Learning Ensemble Model** | 94.1 | 94.51 | 95.64 | 94.26 | 89.01 | 89.6 |
| **Existing DSPM** | 95.13 | 95.86 | 96.79 | 96.15 | 91.4 | 91.57 |
| **Proposed EPBC** | 96.18 | 97.07 | 97.6 | 97.5 | 93.77 | 93.41 |
| **Proposed TCLMCNL** | 96.83 | 97.95 | 98.52 | 97.1 | 95.38 | 95.69 |
| **Proposed MO-UNetDL** | 97.9 | 98.86 | 99.15 | 98 | 97.57 | 97.65 |

Table 9.9 describes the classification outcomes of proposed and conventional methods for two datasets. Evaluation of classification methods is carried out with conventional methods. In comparison to other methods, MO-UNetDL yielded better results in classifying patient data for disease identification than the EPBC, TCLMCNL, Deep Learning LSTM ensemble model, and DSPM.

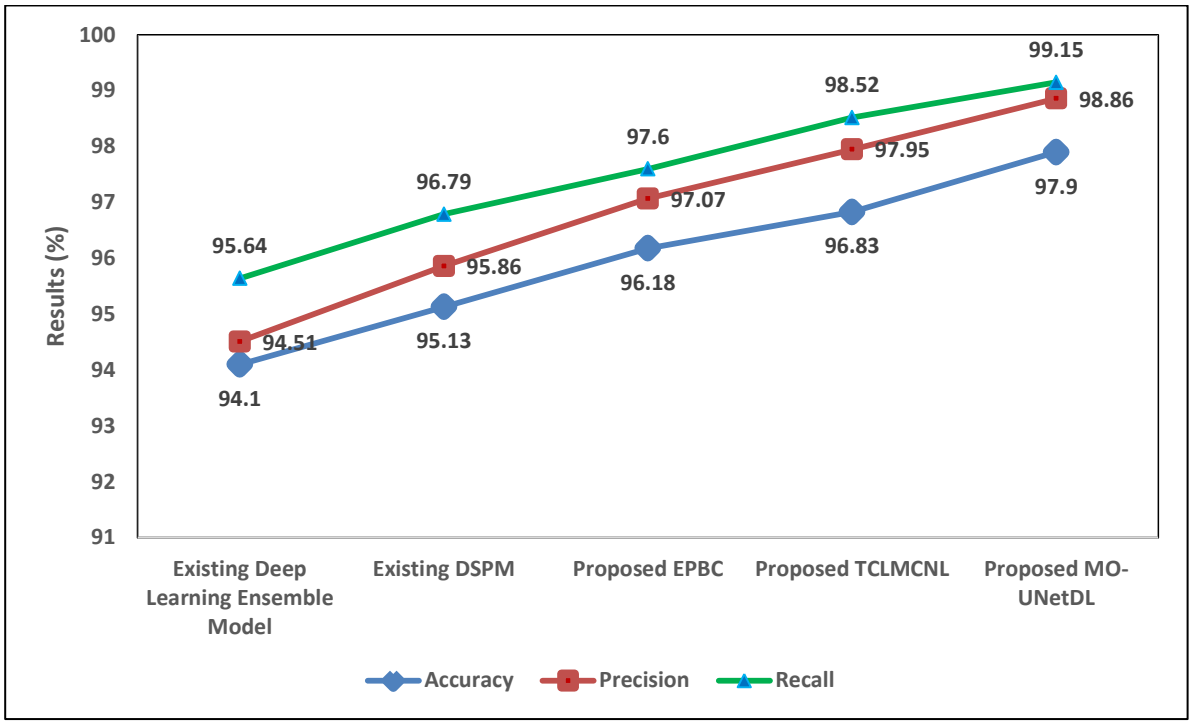


**Figure 9.5 (e) Results of Classification with Preprocessing and Feature Selection for COVID-19 Dataset**

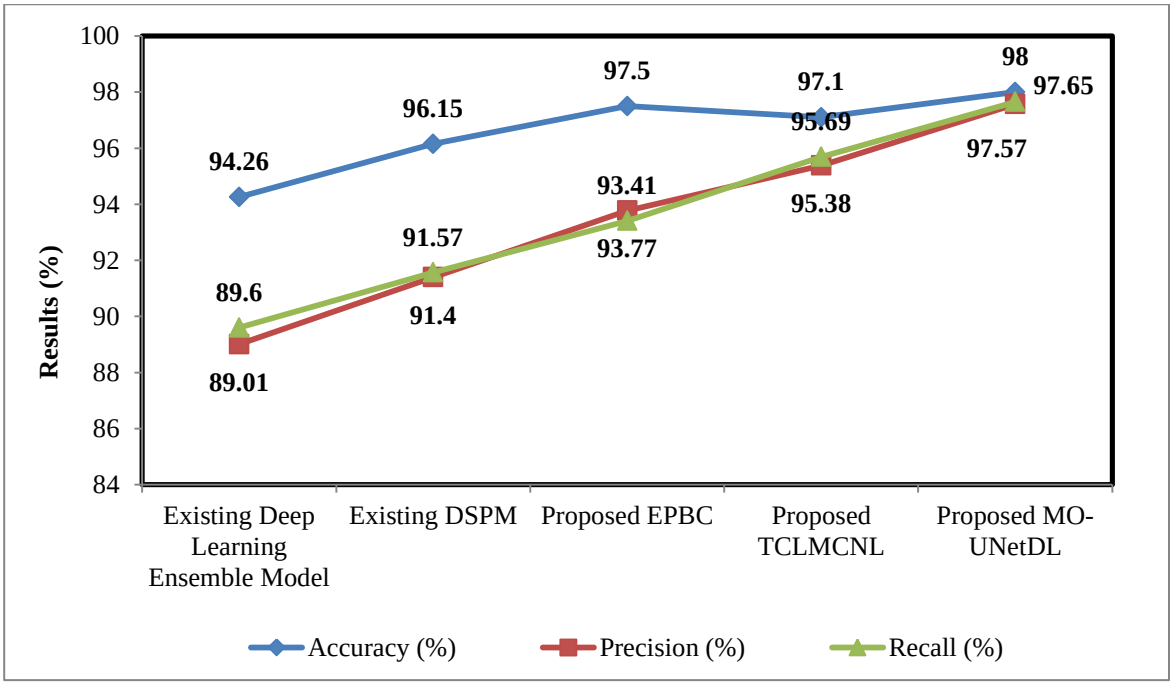


**Figure 9.5 (f) Results of Classification with Preprocessing and Feature Selection for Pneumonia Dataset**

Figure 9.5 (e) and (f) reveal the performance study of classification methods through preprocessing and feature selection processes for both COVID - 19 and Pneumonia datasets. Prior to the classification process, preprocessing is initially performed to eliminate missing and noisy data. Then, feature selection is employed to select pertinent aspects to simply identify the disease. The process of classification through the selected features efficiently enhances the performance of the classification in the MO-UNetDL method compared to other proposed and existing methods. Thus, the results of classification accuracy using the MO-UNetDL method are improved by 3% and 2% compared to existing methods for the datasets COVID-19 and Pneumonia. Additionally, the precision results are improved by 3% and 7% for the MO-UNetDL method, and the recall is improved by 2% and 7% for the COVID-19 dataset and the Pneumonia dataset, respectively.

### 9.5.5 Overall Classification Outcomes

An overall study of classification methods is analyzed under four different conditions: without PP and FS, with PP but without FS, without PP but with FS, and with PP and FS.

**Table 9.10 Overall Comparative Analysis of Classification for COVID-19 Dataset**

| Methods | Accuracy (%) | Precision (%) | Recall (%) |
|---|---|---|---|
| Proposed EPBC w/o PP and FS | 74 | 73 | 73 |
| Proposed EPBC with PP w/o FS | 71 | 74 | 73 |
| Proposed EPBC w/o PP with FS | 73 | 77 | 76 |
| Proposed EPBC with PP and FS | **96** | **97** | **98** |
| Proposed TCLMCNL w/o PP and FS | 77 | 75 | 74 |
| Proposed TCLMCNL with PP w/o FS | 76 | 75 | 75 |
| Proposed TCLMCNL w/o PP with FS | 78 | 78 | 78 |
| Proposed TCLMCNL with PP and FS | **97** | **98** | **98** |
| Proposed MO-UNetDL w/o PP and w/o FS | 80 | 78 | 77 |
| Proposed MO-UNetDL with PP w/o FS | 81 | 79 | 78 |
| Proposed MO-UNetDL w/o PP with FS | 84 | 81 | 81 |
| Proposed MO-UNetDL with PP and FS | **98** | **99** | **99** |

Table 9.10 demonstrates the overall results of the proposed classification methods, including EPBC, TCLMCNL, and MO-UNetDL, for the COVID-19 dataset. Among the three methods, MO-UNetDL with preprocessing and feature selection achieves efficient performance during disease detection. This is because efficient preprocessing and feature selection techniques employed in MO-UNetDL to improve classification performance. Both the presence of preprocessing and the feature selection process enhance the classification result of MO-UNetDL in terms of accuracy (98%), precision (99%), and recall (99%), respectively.

**Table 9.11 Overall Comparative Analysis of Classification for Pneumonia Dataset**

| Methods | Accuracy (%) | Precision (%) | Recall (%) |
|---|---|---|---|
| Proposed EPBC w/o PP and FS | 76 | 78 | 77 |
| Proposed EPBC with PP w/o FS | 79 | 79 | 77 |
| Proposed EPBC w/o PP with FS | 81 | 81 | 81 |
| Proposed EPBC with PP and FS | **98** | **94** | **93** |
| Proposed TCLMCNL w/o PP and FS | 79 | 80 | 79 |
| Proposed TCLMCNL with PP w/o FS | 81 | 81 | 79 |
| Proposed TCLMCNL w/o PP with FS | 83 | 84 | 83 |
| Proposed TCLMCNL with PP and FS | **97** | **95** | **96** |
| Proposed MO-UNetDL w/o PP and FS | 84 | 82 | 81 |
| Proposed MO-UNetDL with PP and w/o FS | 84 | 83 | 82 |
| Proposed MO-UNetDL w/o PP with FS | 87 | 87 | 85 |
| Proposed MO-UNetDL with PP and FS | **98** | **98** | **98** |

The average comparative analysis of three proposed classification methods for the Pneumonia dataset is described in Table 9.11. As observed in the table above, MO-UNetDL yields better classification outcomes in all conditions than the EPBC and TCLMCNL methods. The irrelevant data in both datasets are removed using a preprocessing process. Also, the most prominent features for disease identification are selected to classify the patient data. Through the

preprocessing and feature selection process, the classification of MO-UNetDL is enhanced. The MO-UNetDL with preprocessing and feature selection achieves accuracy of 98%, 98 % of precision, and 98% of recall respectively.

## 9.6 PERFORMANCE OF PREPROCESSING, FEATURE SELECTION AND CLASSIFICATION TECHNIQUES

The overall results of the proposed preprocessing, feature selection, and classification techniques are observed using the COVID-19 dataset and Pneumonia dataset. Both datasets are splited into training and testing sets, where the training set includes 70% of the data, and the testing set includes 30% of the data to estimate model results and their robustness. The aforementioned performance of 70% and 30% split is carried out in each phase, such as preprocessing, feature selection, and classification, using various performance metrics. The following Tables (a) and (b) show the results of preprocessing techniques for COVID-19 and Pneumonia datasets.

**Table 9.12 (a) Results of Preprocessing Techniques for COVID-19 Dataset**

| Methods/Metrics | Training PA (%) | Testing PA (%) | Preprocessing Time (ms) | Error Rate (%) | Space Complexity (KB) |
|---|---|---|---|---|---|
| **Existing VOC-DL** | 69.52 | 67.5 | 6300 | 30.48 | 78.63 |
| **Existing CNN-GRU based Deep Learning Model** | 74.25 | 71.36 | 5960 | 25.75 | 71.25 |
| **Proposed ALRTOHE** | 81.52 | 81.25 | 5462 | 18.48 | 66.25 |
| **Proposed ZMFNE** | 84.63 | 84.36 | 5085 | 15.37 | 62 |

**Table 9.12 (b) Results of Preprocessing Techniques for Pneumonia Dataset**

| Methods/Metrics | Training PA (%) | Testing PA (%) | Preprocessing Time (ms) | Error Rate (%) | Space Complexity (KB) |
|---|---|---|---|---|---|
| **Existing VOC-DL** | 70.89 | 67.52 | 5100 | 29.11 | 74.5 |
| **Existing CNN-GRU based Deep Learning Model** | 76.52 | 72.52 | 4630 | 23.48 | 65.82 |
| **Proposed ALRTOHE** | 84.41 | 79.52 | 3950 | 14.59 | 62.36 |
| **Proposed ZMFNE** | 87.26 | 82.63 | 3700 | 12.74 | 58 |

Thus, the results of training PA are achieved, as testing PA yields 84.63% and 84.36% accuracy for ALRTOHE using the COVID-19 dataset. Additionally, the proposed ALRTOHE achieves a processing time of 5,085 ms, an error rate of 15.37%, and a space complexity of 62 KB for the COVID-19 dataset. Additionally, the training, testing, processing time, error rate, and space complexity of ALRTOHE for the pneumonia dataset are achieved as 87.26%, 82.63%, 3700 ms, 12.74%, and 58 KB, respectively.

**Table 9.13 (a) Results of Feature Selection Techniques for COVID-19 dataset**

| Methods/Metrics | Training FA (%) | Testing FA (%) | Feature Selection Time (ms) | Error Rate (%) | Space Complexity (KB) |
|---|---|---|---|---|---|
| **Existing** $Chi^2$-MI | 79.25 | 76.25 | 6920 | 20.75 | 76.3 |
| **Existing AHEG-FS** | 82.14 | 79.52 | 6420 | 17.86 | 71.25 |
| **Proposed NSPPS** | 85.63 | 82.63 | 5800 | 14.37 | 67.1 |
| **Proposed TSIDFE** | 87.25 | 84.25 | 5345 | 12.75 | 62 |
| **Proposed SCTPP-FS** | 89.25 | 86.25 | 4950 | 10.75 | 56.25 |

**Table 9.13 (b) Results of Feature Selection Techniques for Pneumonia dataset**

| Methods/Metrics | Training FA (%) | Testing FA (%) | Feature Selection Time (ms) | Error Rate (%) | Space Complexity (KB) |
|---|---|---|---|---|---|
| **Existing** $Chi^2$-MI | 82.52 | 77.52 | 6120 | 17.48 | 73.54 |
| **Existing AHEG-FS** | 85.64 | 80.63 | 5530 | 14.36 | 71.36 |
| **Proposed NSPPS** | 87.52 | 84.58 | 4030 | 12.48 | 64.52 |
| **Proposed TSIDFE** | 89.63 | 86.52 | 3360 | 10.37 | 57.63 |
| **Proposed SCTPP-FS** | 91.2 | 88.25 | 3110 | 8.8 | 53.25 |

Table 9.13 (a) and (b) illustrate the overall results analysis of feature selection techniques using the COVID-19 and Pneumonia dataset for 70% (training) and 30% (testing) samples. In comparison to the NSPPS Model, the TSIDFE Technique, AHEG-FS, and $Chi^2$-MI, the proposed

SCTPP-FS achieved improved model performance in both datasets. Experimental results of the proposed SCTPP-FS achieved training FA, testing FA, feature selection time, error rate, and space complexity as 89.25%, 86.25%, 4950ms, 10.75%, and 56.25KB respectively, using the COVID-19 dataset. Moreover, the training, testing, feature selection time, error rate, and space complexity of the proposed SCTPP-FS attained 91.2%, 88.25%, 3110 ms, 8.8%, and 53.25 KB, respectively, using the pneumonia dataset.

**Table 9.14 (a) Results of Classification Techniques for COVID-19 Dataset**

| Classification Methods/Metrics | Training CA (%) | Testing CA (%) | Prediction Time (ms) | Precision (%) | Recall (%) | Specificity (%) |
|---|---|---|---|---|---|---|
| **Existing Deep Learning LSTM ensemble model** | 93.25 | 89.63 | 6730 | 93.62 | 96.21 | 44.52 |
| **Existing DSPM** | 94.25 | 90.31 | 6290 | 94.52 | 94.52 | 46.36 |
| **Proposed EPBC** | 95.25 | 91.12 | 5660 | 96 | 96.15 | 49.63 |
| **Proposed TCLMCNL** | 96.14 | 92.36 | 5230 | 96.67 | 96.36 | 51.25 |
| **Proposed MO-UNet DL** | 96.6 | 93.11 | 4760 | 97.63 | 97.52 | 55.62 |

**Table 9.14 (b) Results of Classification Techniques for Pneumonia Dataset**

| Classification Methods/Metrics | Training CA (%) | Testing CA (%) | Prediction Time (ms) | Precision (%) | Recall (%) | Specificity (%) |
|---|---|---|---|---|---|---|
| **Existing Deep Learning LSTM ensemble model** | 93.2 | 91.3 | 4050 | 95.01 | 96.15 | 46.32 |
| **Existing DSPM** | 95.3 | 92.2 | 3880 | 96 | 96.13 | 48.63 |
| **Proposed EPBC** | 96.2 | 92.5 | 3450 | 96.68 | 96.62 | 51.25 |
| **Proposed TCLMCNL** | 96.4 | 93.4 | 3030 | 97 | 97.68 | 53.12 |
| **Proposed MO-UNet DL** | 97 | 95.6 | 2090 | 97.47 | 98.37 | 57.52 |

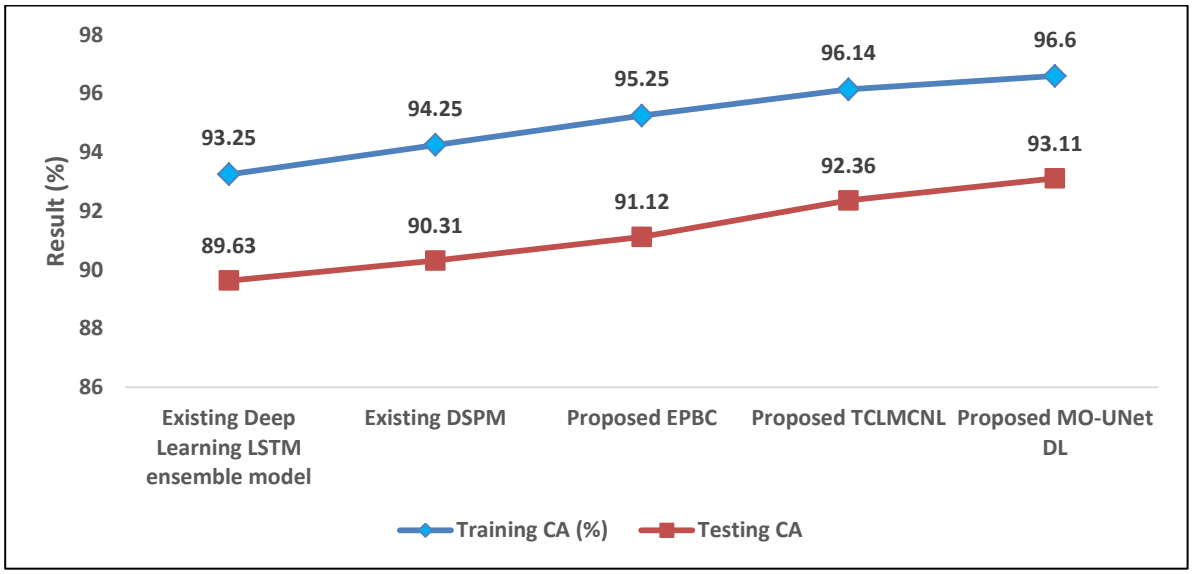


**Figure 9.6 (a) Classification Results of Training/Testing Accuracy for COVID-19 dataset**

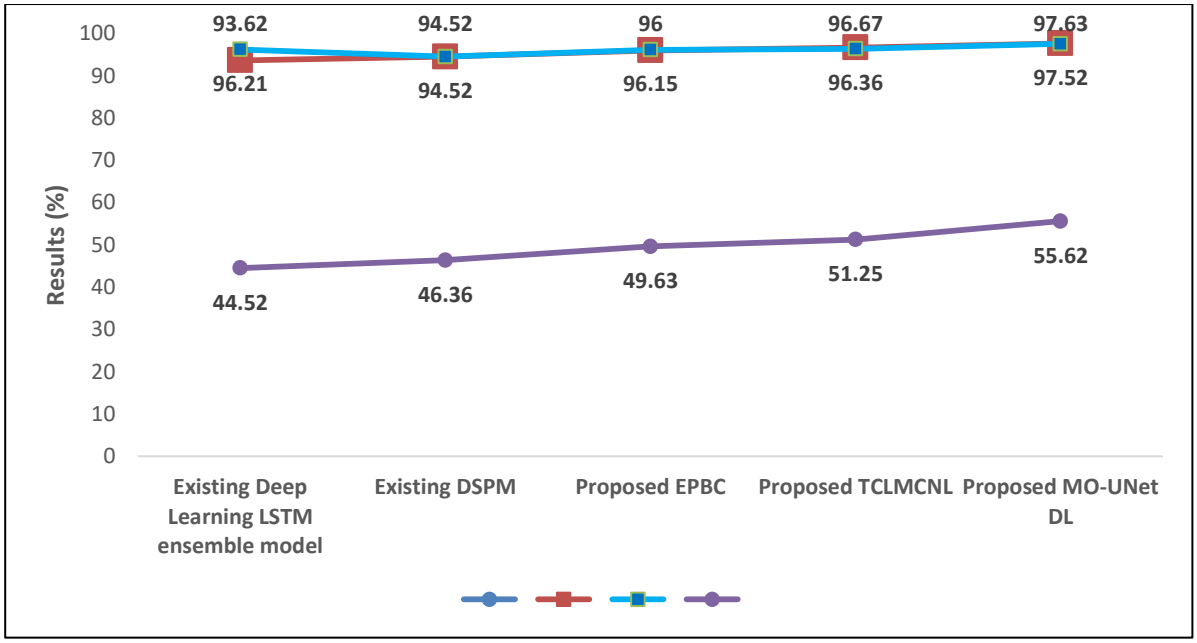


**Figure 9.6 (b) Classification Results of Precision, Recall and Specificity for COVID-19 dataset**

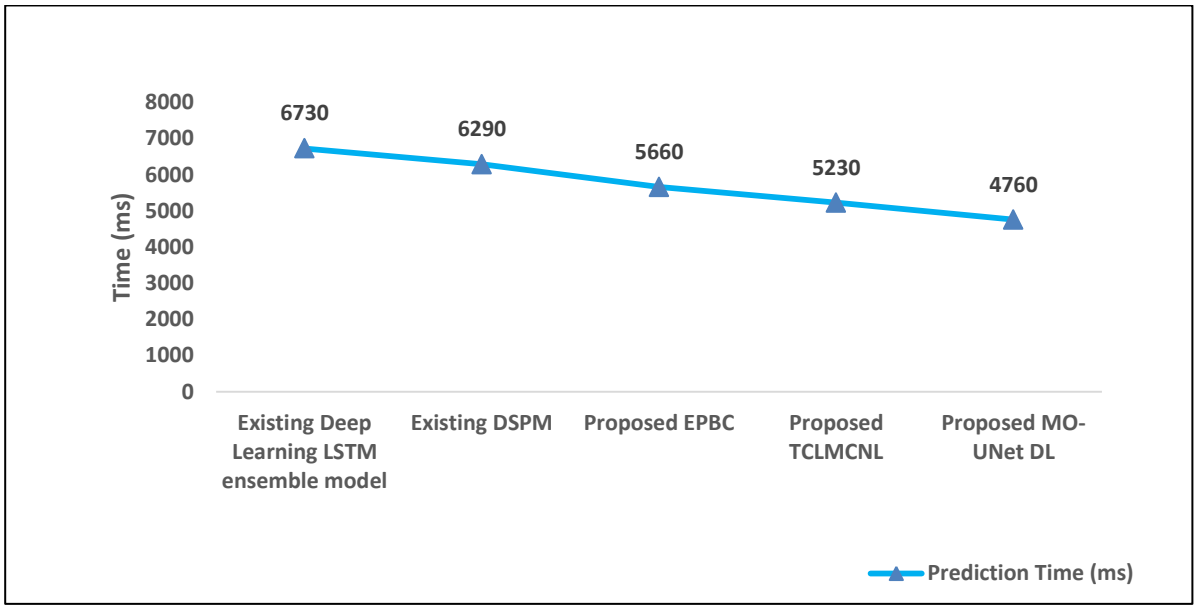


**Figure 9.6 (c) Classification Results of Prediction time for COVID-19 dataset**

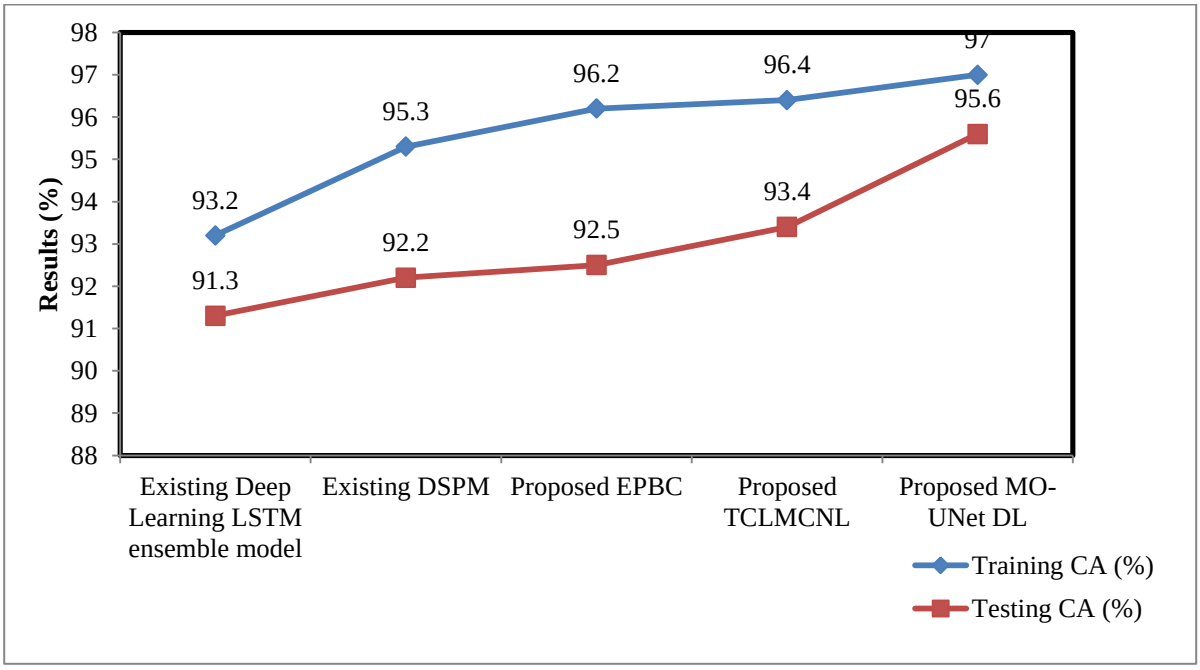


**Figure 9.6 (d) Classification Results of Training/Testing Accuracy for Pneumonia dataset**

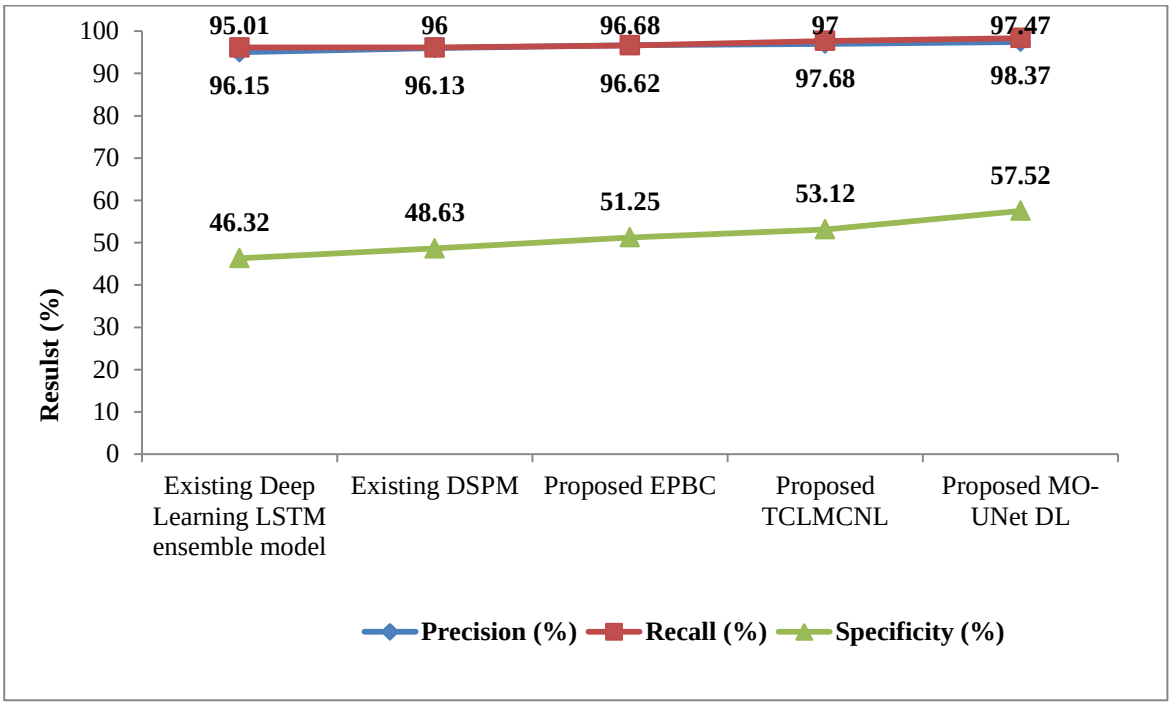


**Figure 9.6 (e) Classification Results of Precision, Recall and Specificity for Pneumonia dataset**

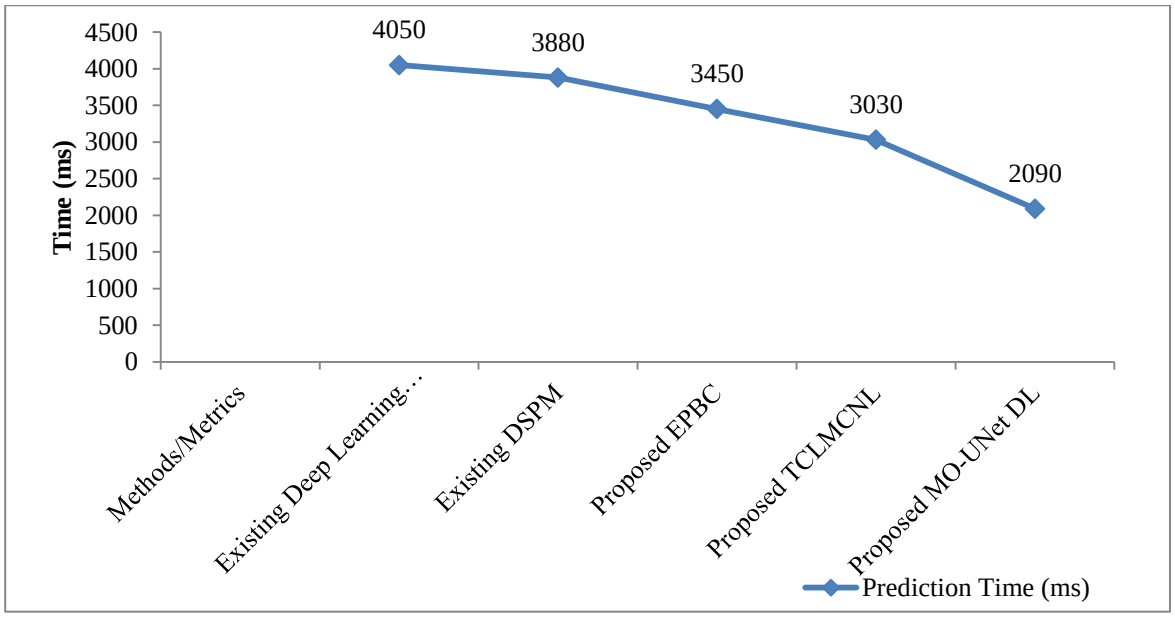


**Figure 9.6 (f) Classification Results of Time for Pneumonia dataset**

The performance outcomes of classification methods for the COVID-19 and pneumonia dataset, with 70% training and 30% testing, are shown in Table 9.14 (a) and (b). Additionally,

Figure 9.6 (a) to (f) provides a graphical representation of the results for both datasets. The validation of the EPBC technique, TCLMCNL technique, and MO-UNetDL technique is carried out by comparing them with a conventional deep-learning LSTM ensemble model and DSPM. According to the results, the proposed MO-UNetDL technique achieved an enhanced outcome compared to other techniques. The results of the MO-UNetDL technique achieved training accuracy (CA), testing accuracy (CA), prediction time, precision, recall, and specificity of 96.6%, 93.11%, 4760 ms, 97.63%, 97.52%, and 55.62%, respectively, for the COVID-19 dataset. Moreover, the MO-UNetDL technique achieved training, testing, and prediction times of 97%, 95.6%, and 2090 ms, respectively, along with precision, recall, and specificity rates of 97.47%, 98.37%, and 57.52% for the pneumonia dataset.

**Table 9.15 Outcome of the Training / Testing Accuracy for the Proposed Classifiers**

| **Classifiers** | **Training/Testing Accuracy (%) 80:20** | | **Training / Testing Accuracy (%) 70:30** | |
|---|---|---|---|---|
| | **COVID-19 Dataset** | **Pneumonia Dataset** | **COVID-19 Dataset** | **Pneumonia Dataset** |
| **EPBC** | 96.18 / 92.65 | 97.5 / 93.54 | 95.25 / 91.12 | 96.2 / 92.5 |
| **TCLMCNL** | 96.83 / 93.52 | 97.1 / 94.25 | 96.14 / 92.36 | 96.4 / 93.4 |
| **MO - UNet** | 97.90 / 94.25 | 98.00 / 96.24 | 96.6 / 93.11 | 97 / 95.6 |

The above TABLE 9.15 shows the results of various Training / Testing accuracy for the proposed classifiers. Where 80:20 Training / Testing accuracy results high performance when compared to the 70:30 ratio.

## 9.7 CHAPTER SUMMARY

The proposed ALRTOHE technique is designed to pre-process the given patient information from the dataset. Though the model gives pre-processing accuracy, data normalization is not performed. Therefore, the ZMFNE technique is developed to perform data normalization during the pre-processing process. The proposed NSPPS technique is used for

feature selection; however, it does not identify more similar features for disease prediction. The proposed TSIDFE Technique is designed to carry out pertinent feature selection with minimal error. However, the minimal number of more correlated features cannot be identified. So another feature selection technique SCTPP is designed, which produces more pertinent features when compared to the other two proposed features selection techniques.

The performance of three classification methods, namely EPBC, TCLMCNL, and MO-UNetDL, is analyzed for two disease datasets: the COVID-19 dataset and the Pneumonia database. A proposed EPBC employing a perceptron binary classifier is introduced to categorize patient information for disease forecasting. However, the training time involved in the method is not reduced further when a huge volume of data is taken into account. The TCLMCNL Technique is designed for classifying data to forecast disease. However, the error optimization is not performed. Therefore, the MO-UNetDL technique is proposed for data classification. The results of the three proposed classification methods are validated with conventional classification methods using classification parameters. Outcomes of classification without preprocessing and feature selection are initially examined. Then, the classification methods with preprocessing, excluding feature selection, are evaluated for five different methods. Also, classification without preprocessing and with feature selection is analyzed. Lastly, the classification results are examined after preprocessing and feature selection. As summarized from the experimental outcomes, the performance of classification is improved in MO-UNetDL compared to other methods, especially in terms of preprocessing and feature selection processes, for both the COVID-19 dataset and the Pneumonia dataset. The next chapter concludes the study and highlights its limitations and recommendations for future work.